



ALMA MATER STUDIORUM
UNIVERSITÀ DI BOLOGNA

SCUOLA DI INGEGNERIA E ARCHITETTURA
DIPARTIMENTO DI INGEGNERIA INDUSTRIALE

CORSO DI LAUREA MAGISTRALE IN INGEGNERIA ENERGETICA

ENERGY ANALYSIS OF A MULTI-FAMILY BUILDING WITH AN INTEGRATED HYDROGEN STORAGE

Tesi di laurea magistrale in
Progettazione di Impianti a Pompa di Calore M

Relatore

Prof.ssa Claudia Naldi

Presentata da

Luca Baccolini

Correlatore

Prof. Fabian Ochs

Dott.ssa Ing. Mara Magni

Appello di marzo 2024

Anno Accademico 2022/2023

ABSTRACT

In the containment of the climate change, since the residential sector plays an important role in the total annual energy consumption, the renewable energy used in buildings needs to be increased, for example with the combined use of photovoltaic panels and energy storage systems. However, while batteries are commonly used for short-term energy storage, their self-discharge rate poses challenges in using them for seasonal need fluctuations and hydrogen energy storage systems (HESS) offer a promising solution. This study, using a MATLAB-Simulink model of a multi-family building located in Innsbruck, Austria, and performing dynamic simulations with different sizes of the electrical components of the building equipment, evaluates the feasibility and efficiency of combining batteries and HESS in residential buildings and furnishes guidance on how to size them.

More in detail, in the Methods chapter, starting from a real project, the MATLAB-Simulink model for the building is presented. Subsequently, the integration of the model with the Heating Ventilation and Air Conditioning (HVAC) plant, is described in two sections, completed with all the required parameters. In the first, the focus is on the subsystem representing the thermal part of the HVAC plant. In the second, instead, the adopted strategy to model the electrical energy generation and storage components of the HVAC plant is exhibited. Finally, the number of the batteries, the number of the hydrogen storage tanks, the number of the electrolyzers, the number of the fuel cells and the number of the additional photovoltaic panels in the cases that have been simulated are listed and the most important performance indicators adopted to evaluate the results are defined.

In the following chapter, the results obtained from the dynamic simulations are analysed and the optimisation strategies that lead to the maximisation of the energy self-production are discussed with particular attention to the energy efficiency which can be achieved in the process.

TABLE OF CONTENTS

INTRODUCTION	1
1. METHODS	6
1.1 Case study	6
1.1.1 General overview of the building	7
1.1.2 Description of the building's energy behaviour	8
1.2 Tools adopted for the simulation	10
1.3 The model of the building	11
1.3.1 Number of thermal zones	11
1.3.2 Geometry	12
1.3.3 Opaque components	13
1.3.4 Windows	14
1.3.5 Shadings	15
1.3.6 Infiltrations	16
1.3.7 Boundary	16
1.3.8 Type of building model for dynamic simulation	16
1.3.9 Internal gains	17
1.3.10 Electrical appliances	18
1.4 The model of the thermal part of the HVAC plant	18
1.4.1 The mechanical ventilation system	18
1.4.2 The Heat Pump	20
1.4.3 Domestic Hot Water Profile	22
1.4.4 The floor heating	23
1.4.5 Auxiliary power consumption due to electrical pumps	24
1.5 The model of the electrical part of the HVAC plant	27
1.5.1 General overview	27
1.5.2 Photovoltaic electrical generation	27
1.5.3 Battery energy storage	29
1.5.4 The hydrogen electrical energy storage system	30
1.6 Cases that have been analysed	33
1.7 Strategy adopted to evaluate the simulation results	35
2. RESULTS AND DISCUSSION	38
2.1 Case 1: the reference case	38
2.2 Case 2: the variation of the size of the energy storage system	45
2.2.1 Effect of the variation of the number of the batteries	45
2.2.2 The variation of the size of the hydrogen storage system	48

2.3 Case 3: the variation of the number of the photovoltaic panels	52
CONCLUSIONS	55
AKNOWLEDGMENTS	58
REFERENCES	59

LIST OF FIGURES

FIGURE 1.1 3D DRAWING OF THE MFB REALISED USING GOOGLE SKETCHUP SOFTWARE, VIEW OF THE SOUTHERN FAÇADE. .	7
FIGURE 1.2 SCHEME OF THE HEAT GENERATION AND HYDRONIC DISTRIBUTION OF THE BUILDING.	8
FIGURE 1.3 SCHEME OF HOW THE SOUTHERN AND EASTERN FAÇADES HAVE BEEN BLENDED. THE LIGHT BLUE LINE HELPS TO VISUALISE THE ORIENTATION OF THE FINAL EQUIVALENT FAÇADE.	13
FIGURE 1.4 MONTHLY ENERGY PROFILES THAT HAVE BEEN ADOPTED FOR THE INTERNAL GAINS.	18
FIGURE 1.5 VENTILATION CONTROL STRATEGY REPRESENTED IN THE FORM OF FLOW CHART.....	19
FIGURE 1.6 SCHEME OF THE SYSTEM INCLUDING THE HEAT PUMP AND THE DISTRIBUTION TOGETHER.....	22
FIGURE 1.7 PROFILE OF THE POWER DELIVERED BY THE HEAT PUMP TO THE BUFFER FOR EACH WEEK.	23
FIGURE 1.8 PLOT OF THE LINEAR CORRELATION OF THE VOLUME FLOW AND THE ELECTRICAL POWER CONSUMED BY THE MAIN PUMP.....	26
FIGURE 1.9 PLOT OF THE LINEAR CORRELATION OF THE VOLUME FLOW AND THE ELECTRICAL POWER CONSUMED BY THE BRINE PUMP.....	26
FIGURE 1.10 PLOT OF THE LINEAR CORRELATION OF THE VOLUME FLOW AND THE ELECTRICAL POWER CONSUMED BY THE SOURCE PUMP.	26
FIGURE 1.11 PRIORITY ORDER FOR THE ELECTRICAL ENERGY STORAGE SYSTEMS AND THE GRID CONNECTION.	27
FIGURE 1.12 HYDROGEN MASS FLOW CONSUMED BY A FUEL CELL AS A FUNCTION OF THE GENERATED ELECTRICAL POWER. .	32
FIGURE 1.13 WASTE THERMAL POWER AND AVAILABLE HEAT RECOVER OF A FUEL CELL AS FUNCTIONS OF THE GENERATED ELECTRICAL POWER.	32
FIGURE 2.1 MONTHLY THERMAL ENERGY NEEDS FOR FLOOR HEATING.	39
FIGURE 2.2 MONTHLY COMPARISON OF THE ELECTRICAL ENERGY NEED DUE TO THE LOADS AND THE PV ENERGY PRODUCTION AND DIRECT CONSUMPTION.	40
FIGURE 2.3 MONTHLY SHARE OF THE LOADS NEED DISTRIBUTED BY SOURCE USED TO PRODUCE THE ELECTRICAL ENERGY.	42
FIGURE 2.4 DYNAMIC PLOT OF THE MASS OF HYDROGEN STORED IN THE TANK, WITH DASHED LINES INDICATING JULY THE 1 ST (RED) AND SEPTEMBER THE 1 ST (BLACK).	44
FIGURE 2.5 MONTHLY SHARE OF THE PHOTOVOLTAIC GENERATION.....	44
FIGURE 2.6 RATIO OF THE TOTAL ELECTRICAL NEED THAT IS COVERED WITH ON-SITE PRODUCTION FROM RENEWABLE ENERGY AND EFFICIENCY OF THE COMBINED STORAGE SYSTEM WITH BATTERIES AND HYDROGEN STORAGE EXPRESSED IN PERCENT AS A FUNCTION OF THE RELATIVE VARIATION OF THE NUMBER OF THE BATTERIES.	45
FIGURE 2.7 ELECTRICAL ENERGY EXCHANGED FROM AND TO THE GRID, CONSUMED BY THE ELECTROLYSERS, GENERATED BY THE FUEL CELLS AND USED FOR CHARGING THE BATTERIES AS A FUNCTION OF THE RELATIVE VARIATION OF THE NUMBER OF THE BATTERIES.	46
FIGURE 2.8 MONTHLY PERCENT RATIO BETWEEN THE DISCHARGED AND CHARGED ENERGY FOR THE BESS EXPRESSED AS A FUNCTION OF THE DIFFERENT SIMULATED SIZES OF THE LATTER.	47
FIGURE 2.9 MONTHLY PERCENT RATIO BETWEEN THE DISCHARGED AND CHARGED ENERGY FOR THE HESS EXPRESSED AS A FUNCTION OF THE DIFFERENT SIMULATED SIZES OF THE LATTER.	47
FIGURE 2.10 DYNAMIC PLOT OF THE MASS OF HYDROGEN STORED IN THE MH TANK IN THE CASE OF THE LARGEST CONSIDERED BESS AND IN THE REFERENCE CASE.	48
FIGURE 2.11 RATIO OF THE ENERGY SELF-PRODUCED FROM PV WITH RESPECT TO THE TOTAL ELECTRICAL NEED EVALUATED ON A YEARLY BALANCE AND EXPRESSED AS FUNCTION OF THE RELATIVE VARIATION OF THE NUMBER OF HYDROGEN STORAGE TANKS, ELECTROLYSERS AND FUEL CELLS.	49
FIGURE 2.12 AVERAGE EFFICIENCY OF THE COMBINED BATTERY AND HYDROGEN ENERGY STORAGE SYSTEM ON A YEARLY BALANCE AND EXPRESSED AS FUNCTION OF THE RELATIVE VARIATION OF THE NUMBER OF HYDROGEN STORAGE TANKS, ELECTROLYSERS AND FUEL CELLS.	49
FIGURE 2.13 DYNAMIC PLOT OF THE STORED MASS OF HYDROGEN FOR THE REFERENCE CASE AND THE CASES +100% AND +200% OF THE SIZE OF THE HYDROGEN STORAGE TANK.	50
FIGURE 2.14 DYNAMIC PLOT OF THE STORED MASS OF HYDROGEN FOR THE REFERENCE CASE AND THE CASE -50%, +50% AND +100% OF THE NUMBER OF THE ELECTROLYSERS.	51

FIGURE 2.15 DYNAMIC PLOT OF THE STORED MASS OF HYDROGEN FOR THE REFERENCE CASE AND THE CASE -50%, +50% AND +200% OF THE NUMBER OF THE FUEL CELLS.....	52
FIGURE 2.16 COMPARISON BETWEEN THE ELECTRICAL NEED CURVE AND THE DIFFERENT PV GENERATION CURVES OBTAINED INCREASING NUMBER OF ADDITIONAL PANELS.	53
FIGURE 2.17 RATIO BETWEEN THE ENERGY EXPORTED TO THE GRID AND THE SUM OF THE ENERGY GENERATED BY THE PVs AND IMPORTED FROM THE GRID IN A YEARLY BALANCE BY INCREASING THE NUMBER OF THE PV PANELS.	54

LIST OF TABLES

TABLE 1 SUMMARY OF THE OPAQUE AND CLEAR AREAS FOR THE SIMPLIFIED BUILDING WITH TYPE, BOUNDARY CONDITION, ORIENTATION AND INCLINATION SPECIFIED.....	13
TABLE 2 SUMMARY OF THERMAL AND OPTICAL PROPERTIES OF THE OPAQUE COMPONENTS.....	14
TABLE 3 DATA USED FOR THE CALCULATION OF THE AVERAGE THERMAL BRIDGE PROPERTIES AND CALCULATED ONES.....	14
TABLE 4 WINDOW OPTICAL PROPERTIES.....	15
TABLE 5 GEOMETRICAL AND THERMOPHYSICAL PROPERTIES OF THE WINDOWS.....	15
TABLE 6 WINTER AND SUMMER REDUCTION FACTORS FOR THE WINDOWS TO TAKE ACCOUNT OF THE SHADINGS.....	15
TABLE 7 MONTHLY CONSTANT TEMPERATURE VALUES OF THE CELLARS AND THE GARAGE.....	17
TABLE 8 PARAMETERS USED IN THE MODEL TO DESCRIBE THE VENTILATION STRATEGY OF THE BUILDING.....	19
TABLE 9 PARAMETERS FOR RADIATOR BLOCK FROM CARNOT LIBRARY.....	24
TABLE 10 SUMMARY OF THE ORIENTATIONS, NUMBER OF MODULES AND PEAK POWER OF THE PV FIELDS INSTALLED ON THE BUILDING ENVELOPE.....	28
TABLE 11 VALUES OF THE PARAMETERS USED IN THE BATTERY BLOCK.....	30
TABLE 12 ELECTRICAL POWER CONSUMPTION, HYDROGEN MASS FLOW AND THERMAL POWER WASTED AND RECOVERABLE ASSOCIATED TO ONE ELECTROLYSER.....	31
TABLE 13 SUMMARY OF THE PARAMETERS OF THE ELECTRICAL PART OF THE HVAC FOR THE REFERENCE CASE.....	33
TABLE 14 SUMMARY OF THE ABSOLUTE AND RELATIVE VALUES ASSUMED BY PARAMETERS OF THE ELECTRICAL PART OF THE HVAC FOR THE DIFFERENT CASES THAT HAVE BEEN ANALYSED FOR THE SIZE OF THE ELECTRICAL ENERGY STORAGE SYSTEM.....	34
TABLE 15 NUMBER OF ADDITIONAL PHOTOVOLTAIC PANELS IN THE DIFFERENT SIMULATIONS THAT HAVE BEEN CARRIED OUT.....	34
TABLE 16 SIMULATION-OBTAINED MONTHLY AND ANNUAL VALUES OF THE ELECTRICAL ENERGY CONSUMPTION OF THE AUXILIARIES AND OF THE TOTAL OF THE LOADS, WITH DETAIL OF THEIR RATIO IN PERCENT VALUE.....	39
TABLE 17 RATIO OF THE PV DIRECT CONSUMPTION WITH RESPECT TO THE TOTAL PV PRODUCTION AND THE NEED FOR THE ELECTRICAL LOADS.....	40
TABLE 18 RATIOS OF THE ENERGY DIRECTLY USED FROM PV OR SENT TO THE STORAGE WITH RESPECT TO THE TOTAL PV PRODUCTION AND OF THE ENERGY DIRECTLY USED FROM PV OR REOBTAINED FROM THE STORAGE WITH RESPECT TO NEED FOR THE ELECTRICAL LOADS.....	41
TABLE 19 RATIO BETWEEN THE ENERGY OBTAINED BY THE BESS DISCHARGE AND THAT CONSUMED FOR CHARGING IT EVALUATED ON A MONTHLY AND ANNUAL BALANCE AND EXPRESSED IN PERCENT.....	42
TABLE 20 MONTHLY AND ANNUAL BALANCE OF THE RATIO BETWEEN THE ENERGY OBTAINED BY THE HESS DISCHARGE AND THAT CONSUMED FOR CHARGING IT EXPRESSED IN PERCENT AND VALUE OF THE MASS OF HYDROGEN PRODUCED BY THE ELECTROLYSERS AND CONSUMED BY THE FUEL CELLS IN KG.....	43
TABLE 21 ANNUAL BALANCE OF THE ENERGY CHARGED AND DISCHARGED BY THE BESS AND THE HESS.....	44
TABLE 22 CALCULATED VALUES FOR THE WINTER RESIDUAL NEED THAT PV GENERATION CANNOT COVER AND THE SUMMER PV SURPLUS PRODUCTION.....	45
TABLE 23 VALUES OF THE YEARLY PV SURPLUS ENERGY AND RESIDUAL ELECTRICAL ENERGY NEED AND OF THE CALCULATED THEORETICAL MINIMUM EFFICIENCY FOR OFF-GRID OPERATION FOR THE DIFFERENT CASES WITH INCREASING NUMBER OF ADDITIONAL PV PANELS.....	53

INTRODUCTION

Amidst the imperative of containing the climate change as much as possible and known that global warming is the consequence of a multiplicity of factors, both natural and human-related, the scientific community agrees that reducing the anthropic component of pollutant emissions is our only feasible opportunity to attain the final target. Within the European Union, the residential sector notably contributes approximately 25% to the overall final energy consumption, thereby playing a significant role in the annual pollutant emissions [1]. To address this, it is fundamental to reduce the demand for fossil-based energy by concurrently raising the efficiency of the buildings and HVAC plants and enhancing the penetration of renewable energy sources.

In the case of new buildings, it is common for them not to depend directly on the consumption of fossil fuels, such as natural gas or oil. Indeed, they usually adopt electrical heat pumps for both space heating and domestic hot water and electric hobs in the kitchens, leading to the exclusive use of electrical energy. Nevertheless, they still indirectly contribute to pollutant emissions by importing at least a portion of the electrical energy from the grid, where fossil fuels are part of the energy mix [2]. As a consequence of this, solar panels, that use photovoltaic (PV) cells to convert the renewable energy source from the Sun into electricity, are already widely installed in buildings to increase the renewable energy consumption ratio. Moreover, the penetration of PV energy continues to experience persistent growth and this trend is substantiated by the fact that PV systems have been subject to substantial cost reductions over the years, becoming one of the most cost-effective energy generators [3]. In addition, the integration of PV modules on building facades as well as on the roof is everyday more frequent and there are studies that suggest how to install them to better exploit their potential [4], including the cases of green roofs and facades, which help with keeping the temperature of the modules in the optimal range for operation [5].

However, the major issue to face when dealing with solar energy lies in its stochastic nature. Although many studies have tried to define prediction strategies for PV, but also wind, energy production, they actually focus on a grid-scale level and can be used to

forecast the need for fossil-based energy production with the primary aim of enhancing the grid stability, for example by limiting frequency oscillations and voltage peaks [6]. When coming to domestic or district applications, the objective becomes maximising the direct use of the renewable energy from the installed PV modules, which also helps to shorten the payback period of the installed technologies since this reduces the energy import from the grid, hence the prediction can help to manage energy more efficiently, but is not sufficient. Indeed, since loads partially depend on the arbitrary behaviour of the occupants and the Sun source is not available in all the day hours and every day in the same way, they cannot be shaped after the PV production curve, thus matching the renewable stochastic production and the buildings' energy consumption is not possible without implementing energy storage systems, that is in other words time-shifting the energy input and its effective consumption [7] [8].

Among all, pumped hydro energy storages represent the most mature and efficient typology of energy storage system, reaching values of round-trip efficiency up to 85%. Their working principle includes pumping water from a lower to an upper reservoir when energy is overproduced, hence storing it in the form of gravitational potential energy, and using a turbine to re-obtain electrical energy when the production is insufficient [7]. In order to realise such a system, a proper installation site must be found, hence this is much more feasible in the form of huge plants rather than for domestic or district applications [9] [10]. In [11], a study on a pico-pumped hydro storage plant for residential buildings has been carried out, concluding that, since the available height and the capacity for water storage are limited, it can be used mainly in service to the grid, for example for peak shaving, rather than for improving the PV production's management. Also, it has been concluded that additional electrical energy storage systems might be required in order to produce better cost saves and, hopefully, a shorter payback time.

On the other hand, battery energy storage systems (BEESs) are the most used in residential buildings and have been studied a lot, so that nowadays they are available in many different types. In the past, lead-acid batteries were the most widely utilised; however, they presented numerous issues, including a short lifespan, the necessity for frequent maintenance and a low energy density. These drawbacks propelled research efforts towards the development of new battery types, though some encountered significant environmental issues or difficulties related to high temperature of operation or safety risks. Nowadays, lithium-ion batteries are exponentially growing popular thanks

to many desired qualities, such as both high energy density and power density, that lead to compact commercial products [12]. In addition, they are getting more competitive also in terms of price, as it is continuously decreasing. According to [13], this could be the consequence of the little influence of the price of the lithium itself on that of the final product, that means that even if lithium price arises, as long as the series production is abundant, lithium-ion batteries' price would continue lowering and their market expanding.

However, self-discharge is the most significant limitation affecting BESS and, despite advancements in emerging types, a conclusive remedy has yet to be found. Consequently, it is advisable to prioritise batteries for short-term energy storage, reserving long-term energy storage to other systems. For example, the combination of batteries and a hydrogen energy storage system (HESS) is suggested in [14], as hydrogen can be produced via electrolysis from renewable energy, stored on a seasonal time-spread and converted again in electricity by using a fuel cell, in a cycle that is completely carbon neutral [15].

More in detail, hydrogen has a huge potential as energy carrier since it has the highest energy per mass unit, yet it has also the lowest volumetric energy density. This results in the necessity for unconventional storage systems, elevating the overall cost of the technology, introducing safety concerns, and diminishing the overall efficiency. For instance, storing hydrogen as compressed gas is the most mature option, but it requires a pressure of about 700 bar in order to store enough mass in an acceptable volume, thus typically 20% of the hydrogen energy is lost in the compression process and safety prescriptions for high pressure vessels must be followed. Furthermore, both liquefaction and physisorption are not alternative solutions. The former is still a very energy-consuming process and can only be applied for short-term storage because of the hydrogen boil-off drawback, the latter is not mature enough for deploying it on a commercial scale, as it has to face issues like low hydrogen density and the requirement for low temperatures. Eventually, chemisorption in metal hydrates emerges as the most viable choice. In particular, the possibility to achieve good gravimetric hydrogen capacities at mild temperatures and pressures allows it to have more acceptable costs and less strict safety concerns at the same time, making it a pragmatic solution for building applications [16].

However, when it comes to round-trip efficiency, it is in general lower than 50% even with metal hydrates [7] [16], so the idea behind the combined use of batteries and HESS

is to store energy to cover the daily demand fluctuations with BEES, that exhibit a better efficiency but also a higher self-discharge rate, and only seasonal variations with the latter. In [17], a single-family house located in Finland and equipped with PVs, batteries and a HESS with metal hydrates storage tank has been presented as case study, in order to evaluate the feasibility of off-grid operation. In this specific example, the authors suggest that the necessity for implementing a hybrid storage system, including both batteries and hydrogen, is the consequence of the choice of the locality, as the extreme latitude makes the building subject to months of light, with PV overproduction, and periods of darkness, when the produced energy is insufficient. Also, they underline that the peak of the consumption comes with the heating load, since in Finland the winter is severely cold, and so there is a seasonal shift between the maximum PV production and the maximum energy consumption. Although this is true, it must be considered that this behaviour applies in general to all the cold localities, where the heating demand prevails on the cooling demand and the latter might be mostly covered with free cooling. Therefore, in the mentioned case study, the impact of the latitude relies in the amplitude of the fluctuations, and, consequently, in the size of the required hybrid system, rather than in the necessity of such a system.

As a consequence of this statement, a multi-family building that will be constructed in Innsbruck, Austria, and equipped with PVs, batteries and a metal hydrate hydrogen storage tank has been considered as case study and analysed with reference to the concept of net-zero energy buildings. According to [18], although the idea of Net-Zero Energy Building (NZEB) was probably born in the late 1970s and early 1980s as a consequence of the oil crisis and has gained particular interest in the latest years in order to reduce the buildings' environmental impact, a unique definition is missing at the moment. In general, papers agree on defining a NZEB as a building capable of producing at least as much energy as it consumes over a yearly balance. Additionally, it is yet fundamental to mention that the on-site generation must be the result of the exploitation of renewable energy sources, such as solar energy, and that the net-zero balance must be achieved acting primarily on the maximisation of the building efficiency, both of the envelope and of the HVAC plant, rather than by just oversizing the renewable energy generation systems.

Stated these principles, a model for the building, integrated with both the thermal and electrical parts of the HVAC, was developed in order to investigate, via dynamic

simulation, which is the impact of varying the size of the electrical energy storage systems on the building's self-consumption of electrical energy and the efficiency of this process. The aim is to provide guidance on sizing the electrical components of the building equipment to maximise the on-site production and use of energy, and hence minimise the energy import from the grid, without compromising the efficiency of the combined battery and hydrogen energy storage system.

More in detail, the model has been realised in the MATLAB-Simulink environment, using carnotUIBK, a dynamic simulation tool developed by the Unit for Energy Efficient Building of the University of Innsbruck, and the carnot library, which is particularly useful for modelling HVAC plants. Subsequently, the building integrated with the HVAC plant sized in the same way as in the starting project has been selected as reference case and hence analysed. Its energy consumption and production have been evaluated and, more in general, its strengths and weaknesses have been discussed. Then, starting from the reference case, the size of the two types of electrical energy storage systems, namely the batteries and the hydrogen storage, have been changed, both increasing and reducing them, and the capacity to self-produce and store the energy for the electrical need and the efficiency of the mentioned process have been observed again. Eventually, different cases with increasing number of additional PV panels have been analysed as well.

All in all, this study is hereby organised as follows. In Chapter 1, the building and the HVAC plant are presented in detail. Also, information about the limits of the software and thus the necessity to simplify the building is pointed out. Then, the building model is described in detail and all the simulation parameters are reported, with particular attention to their variations that indeed represent the cases that have been analysed. In addition, some key performance indicators used to analyse the simulation results are defined. In Chapter 2, the results of the dynamic simulation are described and deeply discussed, in order to produce some guidelines on which choices suit to the idea of increasing both the efficiency and the energy self-consumption of the building coupled with the combined battery and hydrogen energy storage system. Eventually, some possible further developments of this study are suggested.

1. METHODS

The energy analysis presented in this work has been carried out by means of dynamic simulation of a specific building and by modifying the size of the electrical energy storages and generators. Since modelling the building chosen as case study has been the first step to do this, in this chapter, an overview of the building is illustrated in the initial part. Then, it is followed by the modelling tools that have been used, where a specific focus on their limits has been kept. Subsequently, a detailed description of the model is provided, completed with all the parameters that are required for reproducing and simulating it. For sake of clearness, the illustration is divided into three main parts. The first is the building itself, so it includes the number of thermal zones that have been considered, the properties of the envelope, the shadings, the infiltrations, the boundary conditions, the type of the model and the effect of the presence of the occupants, hence the internal gains and the electrical appliances. In the second part, then, the description focuses on the thermal part of the HVAC plant, which means that the models of the ventilation strategy, the heat pump, the need and production of the domestic hot water, the floor heating and the auxiliary power consumption are presented. In the last part of the model description, the focus switches to the electrical energy production and storage devices, hence the photovoltaic panels, the batteries and the hydrogen storage system. Additionally, since their utilisation priority order affects the modelling strategy, it is described as well. Eventually, in the last sections of the chapter, the cases that have been analysed are illustrated and the methods adopted for the evaluation of the results are presented.

1.1 Case study

In this paragraph, the overall description of the original building chosen as case study is provided. In particular, the description is organised into two subsections, the first about the building appearance, which includes its presentation from a geometrical point of view and in terms of the projected use of its floors, and the second with the aim of explaining which technologies the building HVAC plant is expected to be implemented with.

1.1.1 General overview of the building

The case study analysed in this work is a new Multi-Family Building (MFB) that will be built in the following years in the periphery of the city of Innsbruck, Austria. A representation of the building can be observed in Figure 1.1.

As a general overview, the building is composed of 42 flats, 6 per each of the 7 floors destined to be used as student residence and each one having 2 or 3 bedrooms, one bathroom, one kitchen and one external loggia, for an overall floor area of about 50-60 m². Also, on the 2nd, 4th and 6th floor, the common area for acceding to the flats has an external opening leading to a balcony of 22.65 m². The ground floor, instead, is projected to have different common spaces for the students, including learning rooms and fitness area, and presents a reserved local for trash collection. Furthermore, additional service rooms are going to be built on the underground floor, accessible using the main stairs or the elevator, in order to offer a huge bike parking, since this is one of the most popular means of transportation used in the city, a garage with many parking spots for cars and connected to the ground floor through a ramp, a room adhibited as deposit for gardening tools, several cellars and a few technical rooms. To be precise, the underground floor area is larger than that of the other floors, so it is important to mention that only part of the mentioned locals is boundary to the heated area. Eventually, the building is topped by a flat green roof and surrounded by a green area.

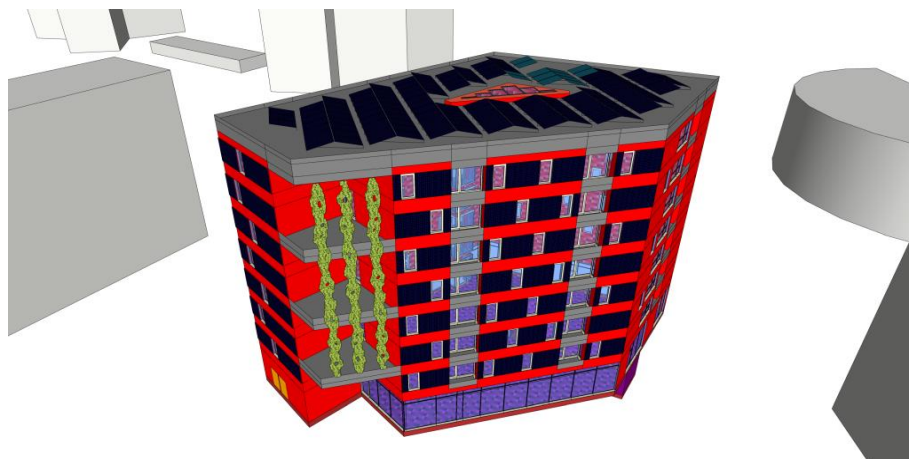


Figure 1.1 3D drawing of the MFB realised using Google SketchUp software, view of the Southern façade.

1.1.2 Description of the building's energy behaviour

From the energy point of view, the building is expected to be certified as a Passive House¹, hence it is well-insulated and equipped with modern technologies, both efficient and capable of exploiting at best heat recovery [19]. More in detail, the thermal energy required by the building for heating as well as domestic hot water (DHW) is produced by an electrical heat pump that uses underground water as external source. Then, water for floor heating is sent to a hydraulic separator before reaching the heated floors, while water for DHW goes to a buffer tank and from there to a different fresh water station for each flat. This one is eventually used, combined with a heat exchanger, which preheats fresh water by means of shower-drain water heat recovery, and a three-way valve, to deliver it at the temperature of 45°C to the taps. For sake of clearness, this part of the HVAC plant is explained in Figure 1.2.

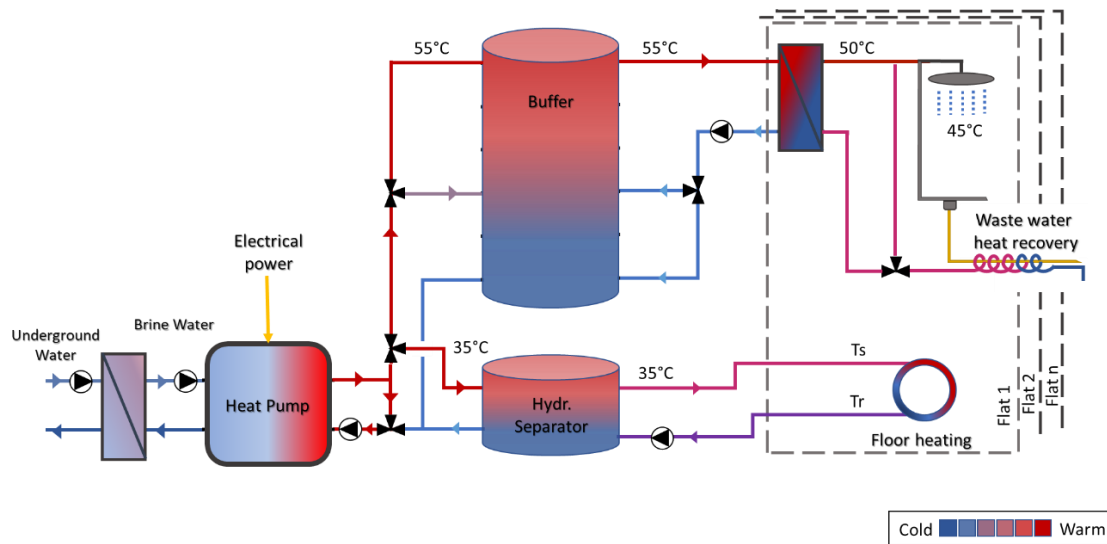


Figure 1.2 Scheme of the heat generation and hydronic distribution of the building.

The availability of underground water, that is well-known to have a stable temperature during the year, higher during the winter and lower during the summer if compared to that of the external air, is exploited also for cooling, so that no additional energy is required, apart from that consumed by the auxiliaries. Furthermore, since the locality

¹ The Passive House Institute is an independent research institute that operates in the field of energy efficient buildings and has developed the so-called Passive House concept. Its employees have realised and constantly update tools for the planning of Passive House buildings, such as the Passive House Planning Package (PHPP), and provide manufacturers in-depth consultancy on product development and optimisation. Furthermore, the Institute acts as an independent testing and certification centre for the achievement of the strict quality requirements of the Passive House Standard by offering professional certifications all over the world.

offers the possibility to often have fresh air, especially during the night, the building is expected to be in large part cooled via free cooling.

In terms of air exchange rate, the building has low infiltrations, so it is equipped with a mechanical ventilation system in order to respect indoor air quality sanitary prescriptions. However, since expelling warm air and reintroducing it cold into the building would raise the heating demand during the winter as well as the cooling demand during the summer, the ventilation system is endowed with a heat recovery section.

In addition to this, the electrical need is obviously incremented by some auxiliaries, such as the circulating pumps and the extraction pump of the underground water, and by the consumption of the electrical appliances used by the occupants.

To meet the requirement of self-generating part of the energy consumed by the building from local renewable energy sources, the building is equipped with PV modules. Nevertheless, as a consequence of the large dimensions of the building and of the idea of applying the NZEB concept to this MFB, even saturating the green roof with PVs is expected to be insufficient to self-produce as much energy as the electrical consumption. Therefore, despite being less cost-effective due to a less perpendicular radiation, PVs are installed also on the façades towards East, West and South directions in a number of modules equal to the maximum acceptable for the fire-protection requirements, while the possibility to have almost only diffuse radiation on the North-East and North-West facades is considered insufficient to make the PV installation valuable enough for exploitation.

Moreover, maximizing the direct use of PV-generated renewable energy within the building is essential to reduce the reliance on the grid electricity and accelerate the payback of the investment. To achieve this, the chosen solution for this MFB has been the installation of a hybrid storage, incorporating both Li-ion batteries and a hydrogen electrical energy storage system (HESS). In further detail, the HESS is composed of polymer electrolyte membrane (PEM) electrolyzers, to produce hydrogen by consuming the surplus of electrical energy, a metal hydride tank to store it as long as necessary and PEM fuel cells to regenerate electrical energy when needed.

However, unlike batteries that work at ambient temperature, the HESS necessitates thermal management. Indeed, firstly, both the electrolyzers and the fuel cells need a cooling loop to be kept in their temperature range of optimal operation and, secondly, the

metal hydrate storage tank requires to be cooled during the loading, as the absorption phase is exothermic, and to be heated to enhance the hydrogen desorption, since this phase is endothermic.

1.2 Tools adopted for the simulation

Dynamic simulations represent a diffuse methodology to further understand the behaviour of buildings and HVAC plants due to the possibility of observing transient phenomena that influence crucial aspects, such as occupant comfort and energy consumption. Indeed, a building represents the meeting point of a multiplicity of variables that follow different physical laws and are influenced by many factors, such as ambient conditions, people behaviour and control strategies. The outcome is a complex union of interacting subsystems that requires advanced tools for modelling and simulation: Simulink (version R2023b), carnotUIBK (version 2.1.5) and carnot (version 8.01), all belonging to MATLAB environment (version R2023b), have been considered to respond to these requirements for the present case study.

More in detail, MATLAB, abbreviation for MATrix LABoratory, is a high-level programming language and interactive environment developed by MathWorks and widely used in many fields, engineering included. Even if it is impossible to mention all its features, for example MATLAB allows the user to perform complex numerical computations efficiently, has a lot of available functions and an easy language to define new customised ones, offers a vast array of toolboxes that extend its capabilities and provide specialised functions and algorithms for specific tasks, supports the integration with many other programming languages and software tools and provides a simple procedure for creating plots, graphs and animations for visualising data and results [20]. However, the Simulink package is the most important feature that MATLAB offers for dynamic simulation, as it consists in a graphical programming environment based on a block diagram interface, hence in an intuitive solution for modelling complex systems [21].

In this environment, carnotUIBK [22], a toolbox for MATLAB Simulink that has been developed by the Unit of Energy Efficient Building of the University of Innsbruck and is available for download at [23], has been used to create the model of the building. Using its Graphical User Interface (GUI), all the input data about the building, namely divided in Geometry, Construction, Gains, Boundary, Thermalzone and HVAC, have been

imported from a precompiled PHPP file and saved into the building object in MATLAB Workspace. Afterwards, the simulation has been started from the GUI, hence the created building object has been used to activate the correspondent blocks of a predefined Simulink file used as template for the building model. It is trivial that this means that the number of available blocks is not infinite: first of all, the maximum number of thermal zones is 10; each of them, then, admits a maximum number of 10 opaque structures, included thermal bridges when present, 5 orientations for the clear components, 5 internal gains profiles, 5 infiltration blocks.

Furthermore, in the template file, the HVAC subsystem is ideal, so both the Simulink library and the CARNOT Toolbox [24], a library of models of the typical technological components of HVAC systems organised in Blocksets and available for download at [25], have been used to adapt it to the present case study.

1.3 The model of the building

1.3.1 Number of thermal zones

In the process of modelling a building for dynamic simulation, when the final aim of the research is well-defined, it serves as a guiding principle in determining the most appropriate simplification strategies, since it enables to discern which aspects of the study can be streamlined without compromising the integrity of the findings and hence it helps to prioritise efforts towards areas that are most pertinent to the study's objectives.

Modelling every room or every flat separately is fundamental when the aim of the research is producing a local analysis of the performance of the building and of the HVAC plant in guaranteeing the comfort of the occupants. Yet, for a study that focuses on the HVAC plant energy analysis, wherein the building is just considered in order to produce a dynamic consumption profile, such a level of detail is unnecessary and a different thermal zoning can be chosen. For instance, every floor or even the whole building could be a different thermal zone.

As a consequence of this statement, although the chosen case study is a large building having 42 flats destined to students and distributed on 7 floors and an additional heated common area on the ground floor, with several rooms for different uses, it can be widely simplified. Also, for the present study, since the objective is analysing the interaction between different parts of the HVAC plant, thus not studying the performance of a single

one, and the building is planned to be certified of Passive House quality, hence it is very well insulated, the detailed knowledge of the slightly different behaviour of every floor is unnecessary and would not justify the inevitable additional modelling effort. Eventually, the building has been modelled as composed of a single thermal zone.

1.3.2 Geometry

In order to use carnotUIBK to do the model of the building by treating it as a single thermal zone, a limit of 10 opaque components, including thermal bridges, and 5 window orientations must be respected. However, the original building has a complex geometry, including 5 façades, a roof, an underground area with rooms having a different destination of use and several loggias and balconies, with windows in more directions, thus a strong simplification is required.

Since carnotUIBK does not have an implemented feature to check if the areas of the building structures can be the external surface of a closed volume, it has been possible to apply the following principle: keeping the correct areas but adapting the orientations.

The first choice has been that of cutting the stairs at the level of the ground floor, so that the latter could actually be a horizontal surface represented by two constructions, one per each of the two neighbour conditions, namely the garage and the other locals, without the heat transfer to the slab floor anymore. At the same time, in the areas of the two types of floor, also those of the vertical walls have been included.

With the same idea, the gross area of each external wall has been calculated as the sum of that of the walls and that of the loggias and balconies insisting on it. With this assumption, the fact that a loggia has two walls perpendicular to the façade, hence being much more in shadow than if these were actually on it, is lost. However, in a Passive House building, solar gains on opaques produce almost no contribution due to the strong thermal insulation and they remain important only for windows, where they can be partially recovered by increasing the shadings on each façade. This has been considered sufficient to make this assumption consistent for the present model.

Since actually some façades are characterised by two U-values due to the presence of PV panels on them, these simplifications were not sufficient to have a number of structures below the limit. As an additional one, the façades in South and East directions have been blended together in a single one, as shown in Figure 1.3.

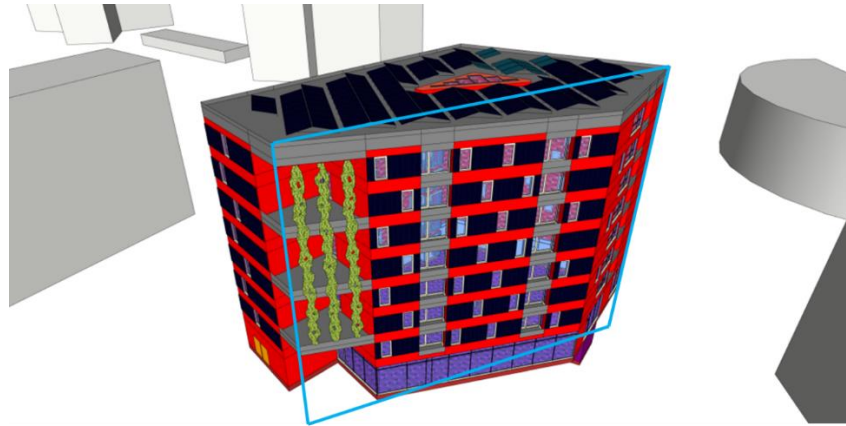


Figure 1.3 Scheme of how the Southern and Eastern façades have been blended. The light blue line helps to visualise the orientation of the final equivalent façade.

When coming to windows, the procedure has been similar and they have been summed together in an equivalent one per each façade of the simplified building plus the roof, leading to a total number of 5 orientations, acceptable for carnotUIBK.

Eventually, Table 1 resumes the areas of the opaque and clear components.

Table 1 Summary of the opaque and clear areas for the simplified building with type, boundary condition, orientation and inclination specified.

Type	Boundary	Deviation from the North	Inclination from the horizontal	Gross wall area	Window area	Net opaque area
Unit		°	°	m ²	m ²	m ²
External wall	Ambient	38	90	499.4	105.4	394.0
External wall	Ambient	164	90	937.4	409.6	527.8
External wall + PV	Ambient	164	90	231.5	0.0	231.5
External wall	Ambient	241	90	177.0	40.1	136.9
External wall + PV	Ambient	241	90	77.5	0.0	77.5
External wall	Ambient	331	90	899.8	349.7	550.1
Roof	Ambient	90	0	546.3	8.7	537.5
Floor	Cellars	90	180	330.6	0.0	330.6
Floor	Garage	90	180	212.6	0.0	212.6

1.3.3 Opaque components

The opaque components that give birth to the 9 structures of Table 1 are two types of external walls, one roof and two types of floor. Specifically, the two types of floor are necessary in order to distinguish the different thermal insulation, lower in the case of garage neighbour and thus leading to a higher U-value. On the other hand, the two different kinds of external wall distinguish the walls with PVs installed on their surface from the normal ones, since the presence of PVs raises a lot the U-value.

In the end, all the thermal and optical properties of the opaque components are resumed in Table 2.

Table 2 Summary of thermal and optical properties of the opaque components.

Construction	U-value	Reduction factor shading	Internal emissivity	External emissivity	Exterior absorptivity
Unit	W/m ² K	-	-	-	-
External wall	0.123	0.7	0.94	0.94	0.65
External wall + PV	0.225	0.0	0.94	0.94	0.65
Roof	0.110	1.0	0.94	0.94	0.65
Floor to cellars	0.154	-	0.94	0.94	0.65
Floor to garage	0.180	-	0.94	0.94	0.65

Eventually, the tenth opaque structure of the single thermal zone's building model represents the equivalent thermal bridge in order to produce the same energy need increase during the year as in PHPP, that is 8324 kWh/a. Since the latter calculates it for every thermal bridge with the formula

$$Energy = L \cdot \Psi \cdot TF \cdot G_t \quad (1.1)$$

where:

- L is the length of the thermal bridge in m;
- Ψ is the Ψ -value of the thermal bridge in W/mK;
- TF is a temperature reduction factor depending on the different neighbour;
- G_t is a factor that converts the calculation in a yearly energy balance, hence expressed in kWh/a;

In the end, the properties of the previous thermal bridges and those of the equivalent one are reported in Table 3.

Table 3 Data used for the calculation of the average thermal bridge properties and calculated ones.

Thermal Bridge	Length	Ψ -value	TF	G_t	Energy need
Unit	M	W/mK	-	kKh/a	kWh/a
Ambient	563.79	0.138	1	81.8	6370
Perimeter	130.53	0.160	0.73	81.8	1254
Floor slab/Basement ceiling	77.70	0.150	0.73	81.8	700
Average	772.02	0.132	1	81.8	8324

1.3.4 Windows

In the building model, the clear components have been grouped together in order to have just one per every orientation and belonging to the normal external walls and to the roof. Also, the glazing parts of the windows on the vertical walls have been considered to be all of the same kind, while the one on the roof has different glass properties, as shown in Table 4.

Table 4 Window optical properties.

Window	g-value	U _g -value	Internal emissivity	External emissivity	Exterior absorptivity
Unit	-	W/m ² K	-	-	-
Vertical walls	0.48	0.52	0.94	0.60	0.65
Roof	0.20	0.80	0.94	0.60	0.65

However, in every façade, the original building has different global window properties due to the fact that the frame fraction might be different depending on the installation in a loggia, on the façade and so on. Eventually, Table 5 summarises all the used values to describe the windows dynamical behaviour, namely the orientation from the North and from the horizontal, the mean U-value of the frame, the Ψ -value of the glazing edge and the average one of the installation borders, the fraction of the glazing area with respect to that of the whole window and the final obtained U-value of the installed window.

Table 5 Geometrical and thermophysical properties of the windows.

Façade	Deviation from the North	Inclination from the horizontal	Mean U _{frame}	Ψ _{Glazing edge}	Average Ψ _{Installation}	Glazing fraction	U _w installed
Unit	°	°	W/m ² K	W/mK	W/mK	%	W/m ² K
North-East	38	90	0.79	0.318	0.012	75	0.700
South and East	164	90	0.79	0.698	0.011	80	0.700
West	241	90	0.79	0.174	0.007	75	0.700
North-West	331	90	0.80	0.452	0.017	75	0.700
Roof	90	0	0.80	0.153	0.015	85	1.030

1.3.5 Shadings

Grouping the windows on every façade has been necessary in order to obtain a maximum number of 5 orientations for the clear components of the modelled building. However, since some of them were on the perpendicular sides of the loggias, the shading reduction coefficients must be increased in order to avoid an overestimation of the solar gains. The values that have been adopted are reported in Table 6.

Table 6 Winter and summer reduction factors for the windows to take account of the shadings.

Façade	Deviation from the North	Inclination from the horizontal	Winter reduction factor	Summer reduction factor
Unit	°	°	%	%
North-East	38	90	55	45
South and East	164	90	50	44
West	241	90	85	34
North-West	331	90	55	33
Roof	90	0	98	98

In addition, it can be noticed that the summer shading reduction factor of the windows on the vertical walls is always lower with respect to the winter one according to the idea that additional mobile shadings will be used by the occupants for temporary sun protection.

1.3.6 Infiltrations

The air exchange rate in h^{-1} is a widely used parameter to describe the infiltrations in a building. In order to calculate it, the Simulink model of the building from carnotUIBK uses the formula

$$n = n_{50} \cdot e_{\text{wind}} \quad (1.2)$$

where n_{50} is the air infiltration rate in h^{-1} when the pressure difference between inside and outside is 50 Pa and e_{wind} is a coefficient that takes into account the protection from the wind.

Since, the building chosen as case study is planned to be constructed with a n_{50} air exchange rate of 0.6 h^{-1} and carnotUIBK automatically sets the e_{wind} coefficient to 0.07, these are the values that have been adopted in the simulation.

1.3.7 Boundary

It is well known that the heat transfer between two volumes depends on the thermal properties of their separating surface, such as the heat transfer coefficient, on the area of it and on the difference between the temperatures of the two volumes. Focusing on the last one, the free-floating temperature inside a building varies depending on the temperatures of the neighbour zones and on the ambient conditions, hence these are the external forces that determine the HVAC plant consumption to maintain the internal temperature of the thermal zone to its setpoint values, that have been considered to be 20°C in winter and 25°C from May till September for the considered case study.

For the time series of the ambient conditions, a weather data file for the locality of Innsbruck, which can be generated again using Meteonorm Software [26], has been introduced in the model. On the other hand, the cellars and the garage, that are the other two neighbours, have been just represented with a different constant temperature every month, as it can be observed in Table 7.

1.3.8 Type of building model for dynamic simulation

Dynamic simulation tools usually allow to select the kind of model of the building depending on the level of detail that the user aims to acquire. carnotUIBK in particular allows to choose the model for the construction and for the thermal zones.

Table 7 Monthly constant temperature values of the cellars and the garage.

Month	Temperature [°C]	
	Cellars	Garage
Neighbour		
January	7.3	-0.2
February	8.8	2.1
March	11.7	6.7
April	14.2	10.8
May	11.2	13.3
June	15.0	16.6
July	17.6	18.7
August	16.6	17.9
September	12.0	14.0
October	14.1	10.6
November	11.0	5.6
December	8.3	1.2

The first choice can be UA, RC or hygrothermal, that means modelling the structures with a U-value and an area, with resistances and capacitances or as in the last one but taking also account of the vapour diffusion. The other choice is between 1*-node or 2*-node model, which is relative to the temperature: in the 1*-node model the user chooses to represent it with a unique value, in the 2*-node temperature is represented with two separate components, namely the radiative temperature and the convective temperature.

In the building model here presented, the building constructions are represented with a RC model and the adopted calculation model for the temperature is the 2*-node.

1.3.9 Internal gains

Since people act as “natural heaters” in the thermal zone and also their actions contribute to heating up the thermal zone, the presence of the occupants in the building often plays a fundamental role in the heating and cooling needs, by reducing the former and increasing the latter.

In order describe this phenomenon, a specific power value, measured in W/m^2 can be used. In the present case study, distinguishing a different value for the winter and the summer internal gains, respectively $2.5 W/m^2$ and $2.3 W/m^2$, has been considered preferable. Since the treated floor area of $2838.4 m^2$ has been used as reference for these values, they lead to the monthly profile of Figure 1.4.

Furthermore, it can be noticed that the switch from the winter to the summer value and the vice versa occur in fixed moments of the year, since the simulation tool is not capable of doing it dynamically. In the end, the summer specific power value is used from June until August, while the winter one is chosen in the other months of the year.

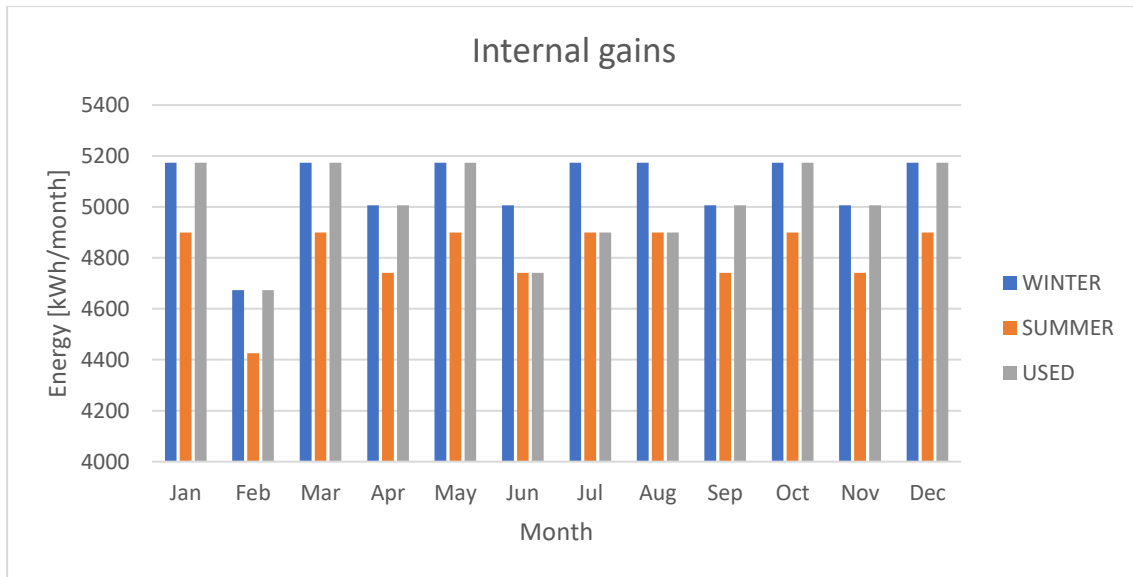


Figure 1.4 Monthly energy profiles that have been adopted for the internal gains.

1.3.10 Electrical appliances

Starting from PHPP, for the modelled building it has been supposed that the yearly energy consumption due to the electrical appliances used in the building is 44576 kWh. Assuming this value, the APCS profile for 2024 [27], after removing the data for February 29th in order to have a regular year of 365 days, has been used as mean to convert the energy value in a power profile with values updated every 15 minutes.

The electrical appliances profile has been then implemented as an additional electrical load in the building model.

1.4 The model of the thermal part of the HVAC plant

1.4.1 The mechanical ventilation system

The ventilation of the building considered as case study is carried out with a double strategy, including both a mechanical ventilation system equipped with a heat recovery section and a free cooling due to window opening.

The control strategy, reported in Figure 1.5 in the form of a flow chart, can be explained as follows. The mechanical ventilation works all the time with a basic air volume flow (\dot{V}_{mec}) and usually adopts the heat recovery section, having the efficiency η_{HR} . However, when the ambient temperature (T_{amb}) is lower than the indoor sensible temperature (T_s) and the latter is higher than the free cooling setpoint ($T_{set,fc}$) of at least 0.5 K, the heat recovery section is bypassed and an additional ventilation (\dot{V}_{fc}) is introduced to take

account of window opening. Furthermore, this ventilation is supposed to continue occurring as long as the indoor sensible temperature is higher than the free cooling setpoint value.

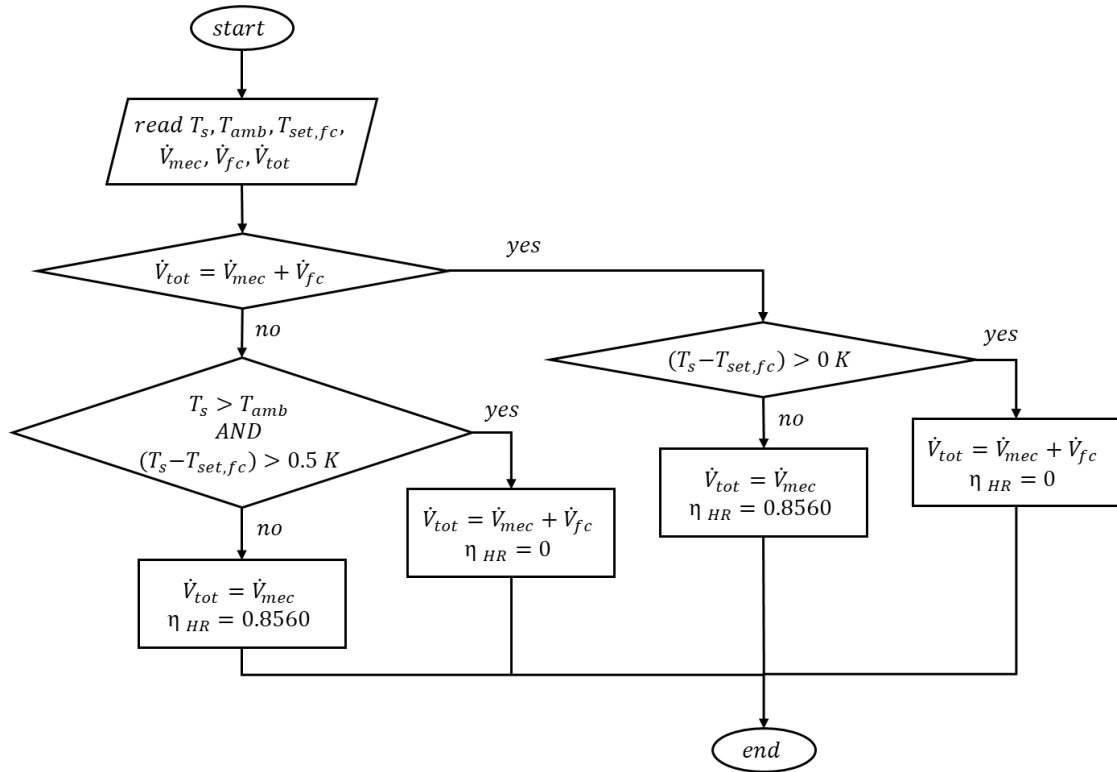


Figure 1.5 Ventilation control strategy represented in the form of flow chart.

In Table 8, instead, the values that have been adopted for the parameters mentioned in the ventilation strategy are listed.

Table 8 Parameters used in the model to describe the ventilation strategy of the building.

Parameter	Unit	Value
$T_{set,fc}$	°C	22
\dot{V}_{mec}	m ³ /h	2489.8
\dot{V}_{fc}	m ³ /h	935.75
η_{HR}	%	85.6

Eventually, the model computes the thermal power associated to the ventilation with the equation

$$\dot{Q}_{vent} = \dot{V}_{tot} \cdot (1 - \eta_{HR}) \cdot \rho \cdot c_p \cdot (T_c - T_{amb}) \quad (1.3)$$

Where:

- \dot{V}_{tot} is the total processed air volume flow, as defined in Figure 1.5;
- η_{HR} is the heat recovery efficiency as defined in Figure 1.5;
- ρ is the air density at the considered instant of time;

- c_p is the air specific heat at the considered instant of time;
- T_c is the convective temperature of the air inside the thermal zone;
- T_{amb} is the ambient temperature at the considered instant of time.

1.4.2 The Heat Pump

The presented building is planned to exploit the availability of underground water at 11°C as the source for the heat pump that produces the water for floor heating and domestic hot water, at a temperature of 35°C and 55°C respectively.

These temperatures can be considered almost constant during the operation of the heat pump due to the fact that the underground water, after a certain depth, is well-known to have a stable temperature during the year and the hot sink temperatures can be maintained using a thermostatic valve. Therefore, it can be expected that the underground water heat pump will work in just two points, one for floor heating and one for domestic hot water, hence having always similar performances in each of them.

As a consequence of this statement, the heat pump has been modelled in an ideal way, starting from the Carnot Coefficient of Performance (COP_{th}), that is the maximum theoretical efficiency that can be achieved for given supply and source temperatures and can be expressed as

$$COP_{th} = \frac{T_{supply}}{T_{supply} - T_{source}} \quad (1.4)$$

The latter has been reduced by a constant coefficient assuming a value between 0 and 1, known as Carnot thermodynamic performance factor (η_C), as suggested by the Austrian norm H5056-1 2023 [28]. However, although the norm also provides average values for it depending on the year of construction of the heat pump, on the source used and on the heat transfer fluid used, for the considered heat pump, the value of η_C has been selected by analysing some commercial products datasheet, that led to adopting 0.48.

Furthermore, for the present model, it has been decided not to model the distribution system, but increasing the energy consumption using a building distribution efficiency has been considered sufficient.

More in detail, normally, the Coefficient of Performance of the heat pump (COP_{HP}) is defined, by focusing on the heat pump loop, as

$$COP_{HP} = \frac{Q_{gen}}{P_{el}} \quad (1.5)$$

where:

- Q_{gen} is the thermal power delivered by the heat pump;
- P_{el} is the electrical power consumed by the heat pump to deliver Q_{gen} .

In presence of thermal losses in the distribution system, the value of Q_{gen} must be higher than that required by the building to maintain the temperature of the thermal zone to the setpoint value ($Q_{building}$) in order to include the unrecoverable thermal losses, hence it is possible to define a global Coefficient of Performance of the heat pump including the distribution losses as

$$COP_{global} = \frac{Q_{building}}{P_{el}} \quad (1.6)$$

It is trivial that the value of COP_{global} cannot be higher than that of COP_{gen} .

In order to pass from COP_{HP} to COP_{global} , it is possible to define the distribution efficiency (η_d) as

$$\eta_d = \frac{Q_{building}}{Q_{generator}} \quad (1.7)$$

Hence it will result

$$COP_{global} = \frac{Q_{generator} \cdot \eta_d}{P_{el}} = COP_{HP} \cdot \eta_d \quad (1.8)$$

That combined with equation (1.4) becomes

$$COP_{global} = COP_{th} \cdot \eta_C \cdot \eta_d = \frac{T_{supply}}{T_{supply} - T_{source}} \cdot \eta_C \cdot \eta_d \quad (1.9)$$

The estimated value of η_d adopted in the model has been 0.97.

In the end, the heat pump has been modelled using the final equation

$$\frac{Q_{building}}{P_{el}} = \frac{T_{supply}}{T_{supply} - T_{source}} \cdot \eta_C \cdot \eta_d \quad (1.10)$$

From which it is possible to evaluate the electrical power (P_{el}) consumed by the heat pump to deliver to the building $Q_{building}$.

Also, from Figure 1.6 and equation (1.10), it is clear that it is possible to evaluate also the power exchanged with the source (Q_{source}) as

$$Q_{source} = Q_{building} - P_{el} = Q_{building} \cdot \left(1 - \frac{1}{COP_{global}}\right) \quad (1.11)$$

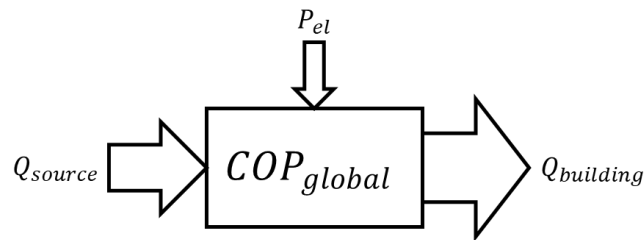


Figure 1.6 Scheme of the system including the heat pump and the distribution together.

In terms of limits, the heat pump has been considered capable of delivering a maximum thermal output power of 35 kW to the building.

1.4.3 Domestic Hot Water Profile

For the domestic hot water, a repeating weekly profile for loading the buffer has been introduced in the model.

The starting point has been the weekly energy consumption of 725.9 kWh, obtained for the chosen building from PHPP and already reduced of the heat recovery from the shower drains. Then, the DHWcalc computer programme, available for download at [29], has been used to produce a weekly energy profile with the same consumption and the latter has been reorganised in order to load the buffer only in the three moments of the day when the domestic hot water request depicts a peak and for the time necessary to produce the sum of all the energy values between the considered peak and the following one.

This strategy led to the profile of Figure 1.7 and aims at representing in a very simple concept: when the buffer is appropriately sized, the need for frequent heating is minimised. Essentially, the heat pump is only activated when the temperature falls below a predetermined setpoint value. This occurrence is more probable to happen during peak demand periods, coinciding with the introduction of larger volumes of cold water into the buffer.

In addition, it must be mentioned that this profile is also used as control signal to give the priority to domestic hot water with respect to the floor heating, since the latter has a big inertia and thus can be stopped for a short time without producing significative changes in the comfort of the occupants.

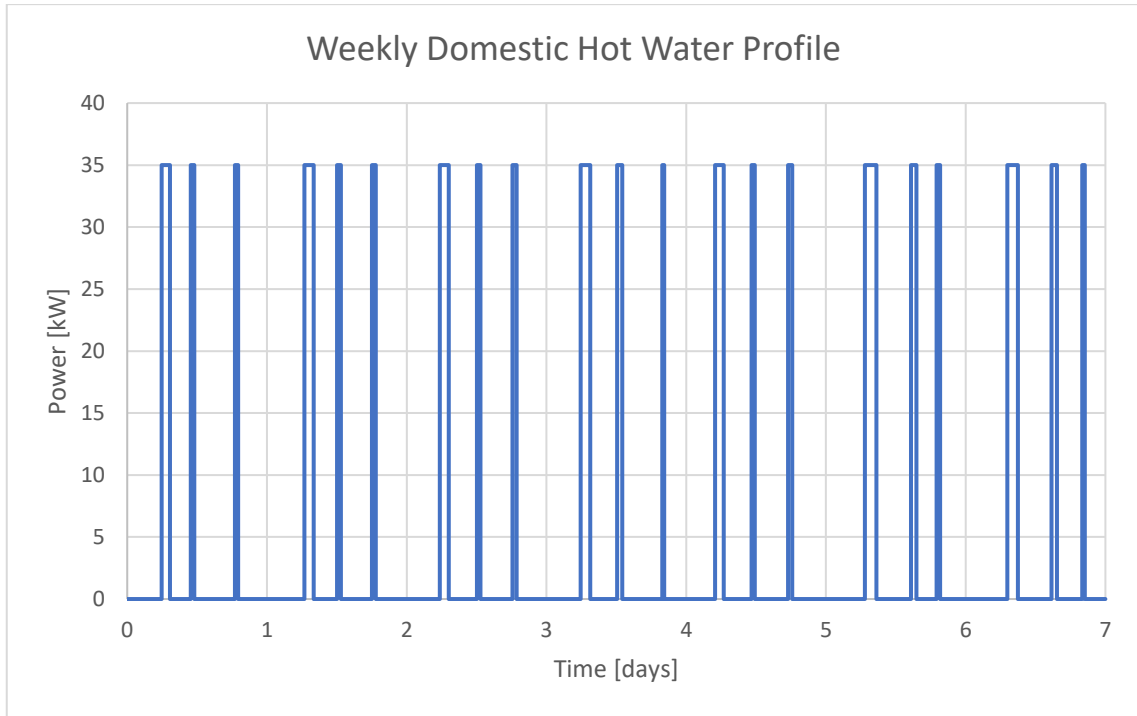


Figure 1.7 Profile of the power delivered by the heat pump to the buffer for each week.

1.4.4 The floor heating

Modelling the floor heating in detail usually requires to define the thermophysical properties of the pipes and of the floors in which these are embedded. However, for the current case study, such a detailed approach is an excessive and superfluous effort if compared to the general scope of the research, that does not definitely focus on it. Therefore, using the approach adopted in IEA Task 44 [30], where a radiator was used to approximate the floor heating, has been evaluated as a more reasonable choice.

In terms of properties required by the correspondent carnot block, the maximum power required by the building has been chosen as nominal power (\dot{Q}_{nom}), the radiator exponent (n) has been kept equal to that chosen in IEA Task 44, the mass*capacity (mc) has been raised proportionally to the ratio of the two buildings treated floor area and the nominal temperature difference has been calculated with the formula

$$\Delta T_{nom} = \frac{T_{s,nom} + T_{r,nom}}{2} - T_{set,winter} \quad (1.12)$$

where:

- $T_{s,nom}$ is the supply temperature to the radiator in nominal conditions;
- $T_{r,nom}$ is the return temperature from the radiator in nominal conditions;

- $T_{set,winter}$ is the setpoint temperature for the heating during winter.

Eventually, the values adopted are resumed in Table 9.

Table 9 Parameters for radiator block from carnot library.

Parameter	Unit	Value
\dot{Q}_{nom}	W	31338
$T_{s,nom}$	°C	35
$T_{r,nom}$	°C	30
$T_{set,winter}$	°C	20
n	-	1.1
mc	GJ/K	1.34

In terms of control strategy, since the supply temperature from the heat pump is considered to be always constant and equal to 35°C, the power instantaneously supplied to the radiator is controlled by regulating the water mass flow with respect to its nominal value, that is obtained with the nominal conditions mentioned above.

However, in some cases, the radiator might be capable of emitting more power to the thermal zone than the maximum value that the heat pump is capable of delivering, hence it could have a return temperature significantly lower than the nominal one. Since this would lead to not respecting the power limit of the heat pump, an additional control calculates the maximum acceptable water mass flow that can be instantaneously produced using the formula

$$\dot{m}_{max} = \frac{\dot{Q}_{HP,max}}{c_{p,w} \cdot (T_s - T_r)} \quad (1.13)$$

where:

- $\dot{Q}_{HP,max}$ is the maximum thermal power that the heat pump is capable of delivering, hence 35 kW;
- $c_{p,w}$ is the water specific heat, assumed equal to 4186 J/kgK;
- T_s is the supply temperature to the radiator, that is 35°C;
- T_r is the return temperature from the radiator, that varies dynamically.

The control finally sets the calculated value as upper limit for the mass flow.

1.4.5 Auxiliary power consumption due to electrical pumps

The final step of the description of the electrical energy consumption associated to the building is usually taking account of the auxiliaries. Estimating in particular the energy consumption of the pumps adopted in the hydronic distribution can be essential when the

aim is studying the building electrical energy management and the electrical energy consumption associated to the heating and domestic hot water is pretty low. In the present case study, in particular, the building is projected to be equipped with high efficiency technologies leading to the obtainment of a low thermal need to be produced by the heat pump. In addition, it will be endowed with a ground water heat pump, which has usually relatively high COP values, hence low electrical energy consumption for given delivered amount of thermal energy.

These characteristics led to the choice of taking into consideration three pumps: the main pump that circulates the water both between the heat pump and the buffer and from the heat pump through the pipes of the floor heating, the extraction pump for the underground water and the circulation pump for the brine water loop. To be precise, the building will be equipped with another pump to send the water from the buffer to the fresh water stations. Yet, the consumption of this pump strictly depends on the instantaneous domestic hot water consumption of each flat, that here was not modelled, hence it could not be taken into account.

The electrical power consumption of the considered auxiliaries has been modelled using linear correlations depending on the processed mass flow. However, the latter was known only for the water used for the floor heating, hence the following equation has been used to calculate it for the cases of the DHW, the brine water and the source water

$$\dot{m} = \frac{\dot{Q}_{th}}{c_{p,w} \cdot \Delta T} \quad (1.14)$$

where:

- \dot{Q}_{th} is the exchanged thermal power;
- $c_{p,w}$ is the specific heat of the water;
- ΔT is the temperature difference to which the fluid is subject.

In terms of values, to evaluate the mass flow to the buffer of the DHW, the value of \dot{Q}_{th} has been taken from the profile of the domestic hot water and the ΔT has been calculated assuming a constant return temperature of 20°C.

On the contrary, in order to evaluate the mass flows of the ground water and of the brine water, the power exchanged at the evaporator has been used as \dot{Q}_{th} and the ΔT has been set to 3K and 5K respectively. Also, it must be noticed that the value of the water specific

heat has been used in all the presented cases: in particular, the amount of ethylenic glycol in the brine water is here supposed to be insufficient to significantly affect the power consumption of the pump.

In Figure 1.8, 1.9 and 1.10 the mentioned correlations are reported in graphs.

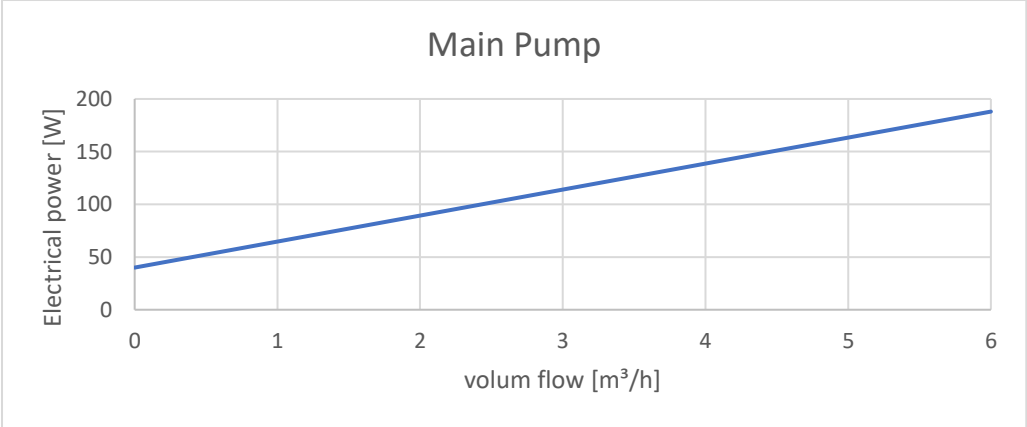


Figure 1.8 Plot of the linear correlation of the volume flow and the electrical power consumed by the main pump.

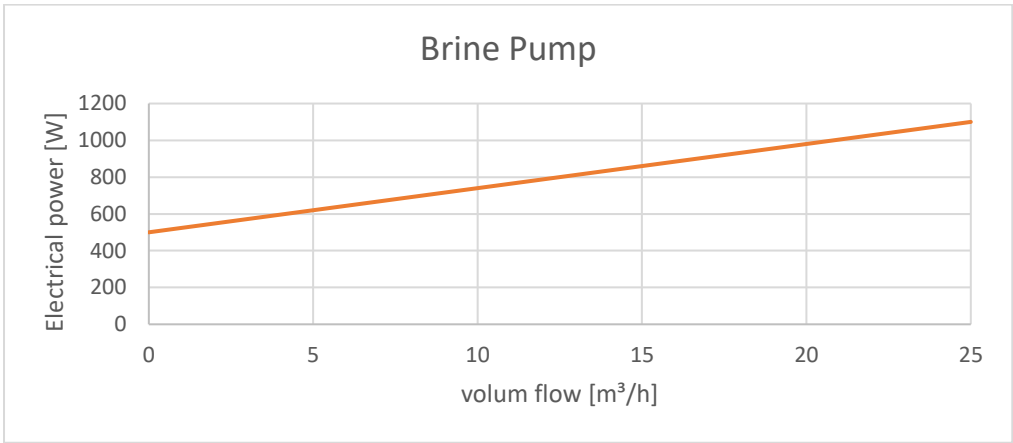


Figure 1.9 Plot of the linear correlation of the volume flow and the electrical power consumed by the brine pump.

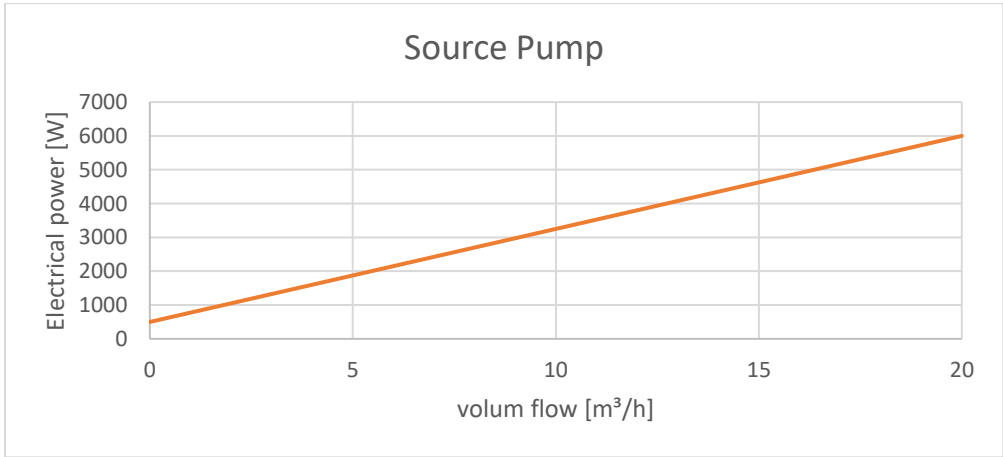


Figure 1.10 Plot of the linear correlation of the volume flow and the electrical power consumed by the source pump.

1.5 The model of the electrical part of the HVAC plant

1.5.1 General overview

Creating the model of the electrical components installed in the building poses several challenges due to their complex behaviour, that can rely on the physical properties of the materials or on some electrochemical reactions that occur and similar reasons. Since the aim of this work is providing a general description of the energy performance in terms of electrical energy management when changing the size of the generators and storages that the building is endowed with, a very detailed description of the electrical equipment is not needed. Therefore, the blocks from the carnot library have been adopted for photovoltaic panels, inverter and batteries, while look-up tables have been preferred to describe the hydrogen energy storage system.

Furthermore, the fact of selecting the hydrogen as a possible solution for addressing the issue of the batteries' self-discharge rate imposes to model the electrical part of the HVAC with a specific order of priority in the energy management. As represented in the scheme of Figure 1.11, the electrical energy produced by the PVs is firstly used to cover the instantaneous loads; then, the batteries have the priority of use and, if not sufficient, the hydrogen storage is used as well. Only as last option, the power can be exchanged via the grid connection.

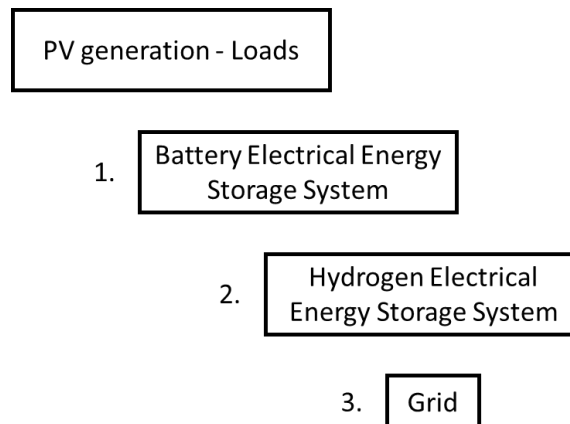


Figure 1.11 Priority order for the electrical energy storage systems and the grid connection.

1.5.2 Photovoltaic electrical generation

As mentioned above, in order to introduce the PV generation in the model, the correspondent block from the carnot library has been used, hence three block parameters, namely the peak power of the generator, the temperature coefficient for the reduction of the

maximum power and the efficiency of the generator, have been set and a weather data bus and a position bus have been connected as input.

More in detail, since the building has PVs on three façades and, on the roof, they are oriented towards East and South, five photovoltaic generator blocks, each one representing the equivalent field of one of the orientations, were sufficient to model the building PV equipment. Since the temperature coefficient for the reduction of the maximum power and the efficiency of the generator have been kept equal to the default value suggested in the block and the surface of the modules has been supposed to be flat, the parameters required for their simulation are those resumed in Table 10, where the peak power of each field has been calculated as

$$P_{peak,field} = P_{peak,module} \cdot N_{module} \quad (1.15)$$

Where:

- $P_{peak,module}$ is the peak power of each module, that has been considered 430 W_p;
- N_{module} is the number of modules installed on the considered field.

Table 10 Summary of the orientations, number of modules and peak power of the PV fields installed on the building envelope.

Field	Azimuth from South	Inclination from the horizontal	Number of modules	Peak power
Unit	°	°	-	W _p
Roof East	-89	30	66	28380
Roof West	91	30	66	28380
East	-43	90	39	16770
South	1	90	38	16340
West	61	90	35	15050

Also, since the PVs act as DC generators, an inverter block has been introduced to take account of the conversion losses. In terms of block parameters, only the AC nominal power has been modified with the value of 60 kW, while the grid parameters, efficiency map, that is the efficiency of the inverter as a function of the ratio between the DC input power and the nominal AC power, and standby power consumption have been set at default values. In addition, the block requires to connect a constant block with the value of the maximum AC power at the correspondent input port, thus a dynamic simulation of the installed PVs has been carried out and the value of 66 kW has been selected, as this represents the maximum instantaneous generated DC power.

However, since the aim of this work is also evaluating the effect of the introduction of more PVs, but it was also known that the number of PV panels on the building could not

be incremented due to the need to respect a minimum distance for the PVs on the roof to avoid mutual shading and due to fire-safety restrictions on the façades, it has been supposed that the neighbourhood of the building offers an unlimited flat area, such as the roof of an industrial building, a green area or a car parking, for the installation of additional PV modules, with the azimuth set to 0° , hence the orientation facing the South, and the inclination of 30° from the horizontal.

Since the inverter parameters for a PV field could require to be adapted depending on its size and the number of modules is indeed the changing parameter of the simulation of the additional field, representing the conversion efficiency with a constant value of 95% is more convenient in this case.

1.5.3 Battery energy storage

Since also for the batteries a predefined block was already available from the carnot library, as mentioned above, using it has been considered the most suitable choice for the purpose of this study.

Nevertheless, a better understanding of the logic behind the block is required. First of all, as the batteries are electrical energy storage systems, this means that they can be either charged or discharged, thus the block accepts both a positive and a negative power value as input, recognising the first one as a charging power and the second one as a load to be covered. Also, even if the batteries normally work with DC current, the carnot block includes in their model also the energy conversion, that must be thus considered when defining the charge and discharge efficiencies.

As a consequence of this, the power signal connected to the input port of the battery block has been defined as the difference of the positive power generated by the PVs and the instantaneous electrical load due to the heat pump, the auxiliaries and the electrical appliances.

However, the block allows also to take account of the typical limits of the batteries, such as the capacity, which is the maximum energy that can be stored, the minimum and maximum state of charge, hence how much of the capacity can effectively be exploited, and the maximum input and output AC powers, which usually represent the maximum C-rate, hence how fast the batteries can be charged and discharged. At completion of these parameter, a standby consumption is considered as well.

From this description, it emerges that it is possible that, in some occasions, the batteries are not capable of processing at all or completely the power signal given as input, hence the carnot block has a specific output signal that represents, when negative, the power of the load that the batteries could not cover and, when positive, the excess of the PV power generation that could not be stored.

When coming to the battery parameters, some of them have been defined as function of the considered number of the batteries ($N_{batteries}$) due to the fact that it is 6 for the base case, but generally variable in this study. Their definition or value is resumed in Table 11, where it can also be noticed that the efficiency of charge and discharge is the product of two values, the first representing the efficiency of the battery itself the second the efficiency of the required conversion from AC to DC or vice versa.

Table 11 Values of the parameters used in the battery block.

Parameter	Unit	Definition/Value
Capacity	kWh	$4.8 \cdot N_{batteries}$
charge and discharge efficiency	-	$0.98 \cdot 0.958$
Max state of charge	-	1
Min state of charge	-	0.7
Max AC power in	W	$4.8 \cdot 10^3 \cdot N_{batteries}$
Max AC power out	W	$-Max AC power in$
Standby power	W	22.5

1.5.4 The hydrogen electrical energy storage system

The hydrogen system that is planned to be installed in the building, in its basic form, is a commercial product composed of 10 electrolysers, to produce hydrogen from PV overproduction when the batteries cannot store it, one metal hydrate storage tank, for storing the produced hydrogen, and 2 fuel cells to reproduce electrical energy when the PV production and the batteries discharge are not sufficient to cover the load. However, the effect of a different sizing of the hydrogen storage system is another aspect studied in this work, hence the number of its components has been kept able to vary.

In order to do this, it has been assumed that:

- the components of the HESS can be treated as modular and, when more than one, installed in parallel;
- both the electrolysers and the fuel cells can only work at fixed point (for the real building chosen as case study this is planned to be true only for the electrolysers);

- when more than one electrolyser or fuel cell are installed, they can work separately, hence also only part of them, in order to be more flexible in the power absorbed or delivered.

These choices, then, allowed to model just one of each component and use the number of the activated ones as a multiplication coefficient to scale up the associated variables.

For the hydrogen storage, since a metal hydrate storage tank has a very different behaviour depending on the adsorbing material, and the latter was not known, it has been modelled as totally ideal, by simply evaluating the integral of the hydrogen mass flow, with this assuming positive values when hydrogen is produced by the electrolysers and negative values when it is consumed by the fuel cells. The only non-ideal features that have been introduced in the model have been the maximum and minimum acceptable mass of the stored hydrogen in the tank, which are used to stop operation of the electrolysers and fuel cells respectively. This choice, however, inevitably led to the loss of the fundamental thermal integration that the metal hydrate storage tank requires for working, that includes a cooling need for adsorbing the hydrogen, a heating loop for the discharging phase and delays of operation, mainly associated with the heat capacity of the metal porous bed.

With regard to the electrolyser, it has been modelled as capable of consuming the electrical power P_{EZ} , increased by the inverse of the efficiency of the AC/DC converter $\eta_{converter}$, to produce the hydrogen mass flow \dot{m}_{H_2} and the waste heat of $\dot{Q}_{th,EZ}$, with the recoverable part $\dot{Q}_{th,rec,EZ}$. The values of these parameters are listed in Table 12.

Table 12 Electrical power consumption, hydrogen mass flow and thermal power wasted and recoverable associated to one electrolyser.

Parameter	Unit	Definition/Value
P_{EZ}	W	2400
\dot{m}_{H_2}	kg/s	$1.25 \cdot 10^{-5}$
$\dot{Q}_{th,EZ}$	W	600
$\dot{Q}_{th,rec,EZ}$	W	250
$\eta_{converter}$	-	0.95

On the contrary, the modelling strategy chosen for the fuel cell has been that of using a look-up table as function of the generated electrical power to describe its behaviour using the information from datasheet and then, since they work at fixed point, to enter this look-up table with the constant value of the generated power, that is 5000 W. This value is eventually reduced by the inverter efficiency of 0.95 when delivered to the building. The look-up tables that have been obtained from datasheet and adopted in the model,

respectively for the hydrogen mass flow consumption and for the thermal power produced and recoverable, are shown in Figure 1.12 and in Figure 1.13.

Eventually, the control strategy to decide how many electrolysers and fuel cells using every time is composed of the following steps: firstly, the electrical power is divided by the power of the fixed point at which they work, then the number is rounded down to the first integer and finally the number is limited between zero and the maximum number of components of the considered case study.

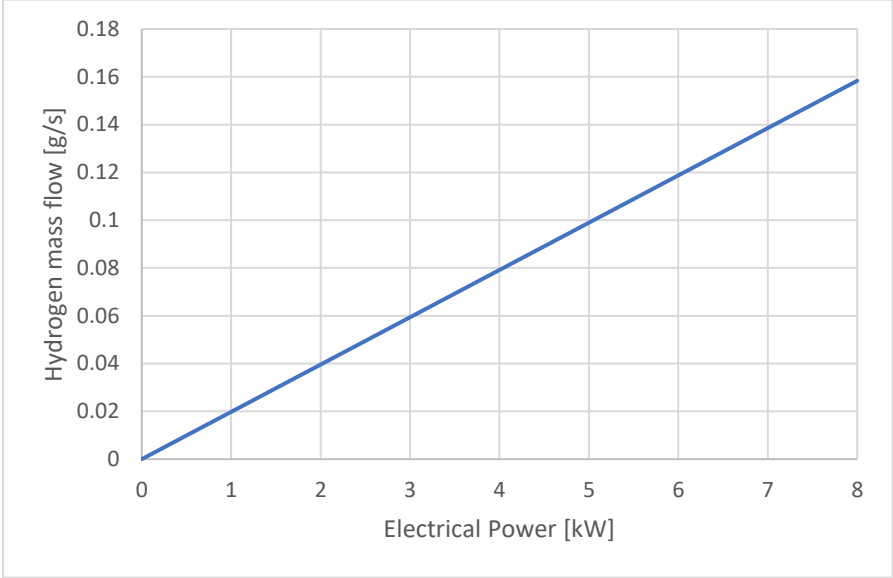


Figure 1.12 Hydrogen mass flow consumed by a fuel cell as a function of the generated electrical power.

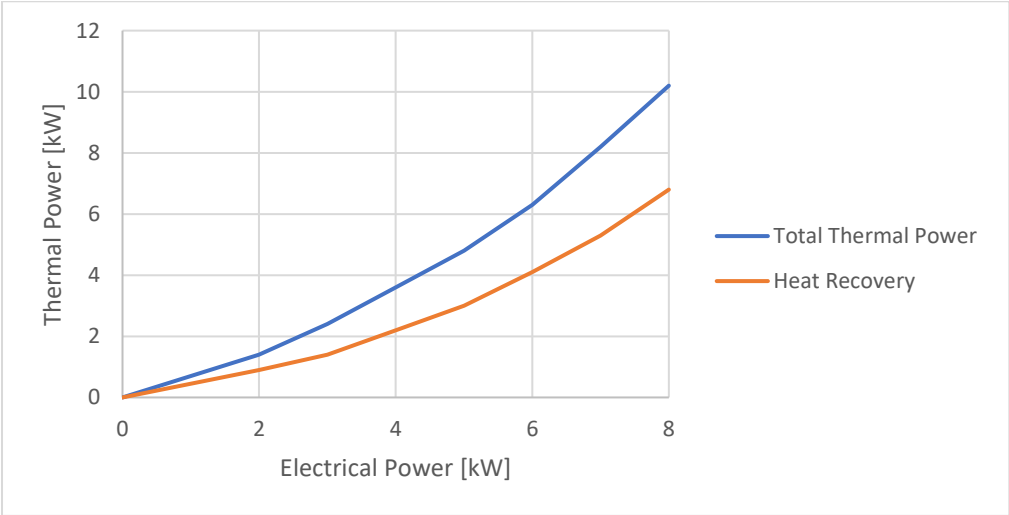


Figure 1.13 Waste thermal power and available heat recover of a fuel cell as functions of the generated electrical power.

1.6 Cases that have been analysed

Since the model has been realised starting from a real project, this has been chosen as reference case and has been studied in detail to understand which are the main improvements that it would be interesting to achieve in its energy management. More in detail, first of all, the variable parameters of the model regarding the electrical part of the HVAC plant of the building have been set according to the mentioned project, and can be found in Table 13; then, an annual dynamic simulation has been carried out.

Table 13 Summary of the parameters of the electrical part of the HVAC for the reference case.

Parameter	Value
Number of the batteries	6
Number of the hydrogen storage tanks	1
Number of the electrolysers	10
Number of the fuel cells	2

The main outputs that have been calculated have been the need of electrical energy for the heat pump, providing thermal energy both for space heating and domestic hot water, the electrical appliances and the auxiliaries. Also, additional results produced by the dynamic simulation have been the energy produced by the photovoltaic panels installed on the roof and on the façades of the building and how this energy is used, hence how much energy is directly consumed by the electrical loads and how much needs to be stored, with distinction between the amount accumulated using the batteries and that stored by hydrogen energy storage system. These variables have been used to understand how the two storages were used and which were the weaknesses to focus on.

In the following part, the effect of the single variation of each one of the mentioned parameters has been studied. The first that has been changed has been the number of batteries and since they have the priority on the use of the hydrogen storage system, the interaction between the two has been studied together with the potential of increasing the energy self-production. Subsequently, the size of the hydrogen storage tank, the number of the electrolysers and finally the number of the fuel cells have been changed and the effect that these parameters have on the use of the hydrogen system has been analysed.

In the end, the absolute values (p_i) adopted for the parameters of Table 13 in the different simulations are resumed in Table 14. In addition, the relative value ($p_{i,rel}$) with respect to the reference case ($p_{i,ref}$), calculated as:

$$p_{i,rel} = \frac{p_i - p_{i,ref}}{p_{i,ref}} \cdot 100 \quad (1.16)$$

has been reported as well.

Table 14 Summary of the absolute and relative values assumed by parameters of the electrical part of the HVAC for the different cases that have been analysed for the size of the electrical energy storage system.

Parameter varied	p_i	$p_{i,rel}$
Number of the batteries	0	-100%
	3	-50%
	9	+50%
	12	+100%
	15	+150%
	21	+250%
	34	+467%
	48	+700%
Number of the hydrogen storage tanks	0	-100%
	2	+100%
	3	+200%
	4	+300%
	8	+700%
Number of the electrolysers	0	-100%
	5	-50%
	15	+50%
	20	+100%
Number of the fuel cells	0	-100%
	1	-50%
	3	+50%
	6	+200%

Eventually, the number of the PV panels has been changed in order to study how the building responds to an increased production of electrical energy and to understand which are the main guidelines that should be followed in doing it. Since the additional PVs could not be installed on the building due to the need to respect fire-safety prescriptions on the building façades and to avoid the mutual shading of the panels on the roof, the presence of an additional area, available for hosting extra PV panels directed to the South and with 30° of inclination, has been supposed. In Table 15, the number of the additional PV panels of the simulations that have been carried out is listed. Yet, in this case, since having additional PVs in different directions produces different results and the building has already panels in multiple orientations and inclinations, the definition of a relative variation for the number of them has been avoided because a unique reference value could not be identified.

Table 15 Number of additional photovoltaic panels in the different simulations that have been carried out.

Parameter varied	p_i
Number of additional PV panels	10
	30
	60
	90

1.7 Strategy adopted to evaluate the simulation results

In order to evaluate what happens to the energy production and self-consumption in the coupling of the building and the HVAC plant, with the latter in the reference case and with different sizes, the first analysis has been based on energy balances. All the most important energy variables, both in terms of energy production and consumption, included the energy exchanged with the grid, stored by the batteries and by the hydrogen storage system, but also the mass of hydrogen produced by the electrolyzers, stored in the ideal metal hydride tank and consumed by the fuel cells, have been post-processed in order to produce monthly and annual balances.

In addition, some performance indicators, have been defined for different purposes, such as evaluating the capacity of the building integrated with the HVAC plant to store the energy produced by the photovoltaic panels, describing how able it is to self-produce the energy that it consumes.

The first of them is the ratio between the energy directly used from the PV generation, both to cover the consumption of the loads or absorbed by the combined battery and hydrogen energy storage system, with respect to the total PV production. This parameter is used to indicate how able is the building coupled with the storage system to absorb the on-site electrical generation from solar energy, hence how much it is able to avoid exchanging energy with the grid, and can be expressed with the formula

$$\text{ratio of absorption of PV generation} = \frac{E_{PV,direct} + E_{BESS,charge} + E_{EZ}}{E_{PV,tot}} \quad (1.17)$$

where:

- $E_{PV,direct}$ is the part of the energy produced by the PVs that is directly consumed by the electrical loads;
- $E_{BESS,charge}$ is the energy produced by the PVs that is used to charge the batteries;
- E_{EZ} is the energy produced by the PVs that is absorbed by the electrolyzers to produce hydrogen;
- $E_{PV,tot}$ is the total energy produced by the photovoltaic panels.

Further to this, a similar parameter, the ratio of self-produced energy, is used to indicate how much of the energy need is covered with energy coming, directly or previa storage, from the PVs. In this case, it is defined as

$$\text{self – produced energy ratio} = \frac{E_{PV,direct} + E_{BESS,discharge} + E_{FC}}{E_{Loads}} \quad (1.18)$$

where:

- $E_{PV,direct}$ is the part of the energy produced by the PVs that is directly consumed by the electrical loads;
- $E_{BESS,discharge}$ is the energy to cover the electrical need that is produced from battery discharge;
- E_{FC} is the energy to cover the electrical need that is produced from the fuel cells by consuming the stored hydrogen;
- E_{Loads} is the total electrical need due to the electrical loads.

Moreover, another performance indicator, namely the ratio between the energy discharged and charged by one of the storage systems, has been used for different purposes, depending on the way in which it has been calculated. In general, it is defined by the formula:

$$\text{ratio of discharge/charge} = \frac{E_{discharge}}{E_{charge}} \quad (1.19)$$

where:

- $E_{discharge}$ is the energy obtained from the discharge of the storage during the period of calculation;
- E_{charge} is the energy used to charge the storage during the period of calculation.

When the ratio is calculated on a period of time long enough to include a high number of closed cycles of charge and discharge, such as during one year, it will always assume the same value, which can be defined as the average efficiency of the considered storage. On the contrary, on shorter periods, it has a more variable value and, the more it is close to the annual value, hence to the average efficiency, the more it means that the storage is used frequently. Therefore, it can be used to distinguish in which months of the year the considered storage is used more for a short-term energy shift and when it is used as a seasonal energy storage system.

Lastly, an average efficiency for the combined battery and hydrogen energy storage system ($\varepsilon_{B\&H\,ESS}$), calculated on annual base, is defined by the formula

$$\varepsilon_{B\&H\,ESS} = \frac{E_{BESS,discharge} + E_{FC}}{E_{BESS,charge} + E_{EZ}} \quad (1.20)$$

where:

- $E_{BESS,discharge}$ is the energy to cover the electrical need that is produced from battery discharge;
- E_{FC} is the energy to cover the electrical need that is produced from the fuel cells by consuming the stored hydrogen;
- $E_{BESS,charge}$ is the energy produced by the PVs that is used to charge the batteries;
- E_{EZ} is the energy produced by the PVs that is absorbed by the electrolyzers to produce hydrogen.

Eventually, in addition to the monthly and annual energy balances and the mentioned performance indicators, in some cases the dynamic plot of the mass of hydrogen stored in the tank has been useful for a better understanding of the behaviour of the hydrogen storage system.

2. RESULTS AND DISCUSSION

In this chapter the results of the simulation are presented and analysed. Starting from the reference case, firstly, the building need of electrical energy and the production of the photovoltaic panels are described, so that the amount of energy that is directly used from PV and that amount which requires to be stored and discharged in a subsequent moment are evaluated; secondly, the behaviour, and hence the performance, of the energy storage system is discussed and the weaknesses which can be improved are pointed out. Subsequently, the parameters which define the size of the electrical components of the HVAC plant, namely the number of the batteries, the number of the hydrogen storage tanks, the number of the electrolysers and the number of the fuel cells, are progressively modified in order to understand how their variation influences the energy performance of the building. Eventually, under the hypothesis of being able to install an additional PV field, the effect of a growing size of the latter on the energy production and on the behaviour of the combined storage with batteries and hydrogen storage is discussed.

2.1 Case 1: the reference case

The initial simulation that has been carried out involved the building model integrated with the HVAC system without any size modification. This was useful to evaluate the starting point of the further changes, hence the reference case.

Thanks to the strong insulation, the building has a heating need of thermal energy for floor heating of 34152 kWh/a, that corresponds only to 12.0 kWh/m²a and is produced by the heat pump. By observing the monthly values for the latter, expressed in kWh/m² in Figure 2.1, it can be noticed that the heating season mainly occupies the period of time between November and March, with a neglectable value of thermal energy need already in October.

In terms of electrical energy consumption, the three types of loads of the building, namely the electrical appliances, the heat pump and the auxiliaries, give birth to a monthly profile of the need that is higher during the winter and lower during the summer. In addition, as shown in Table 16, the importance of estimating the power consumed by the auxiliaries is confirmed in the results, as it contributes 17-19% to the total loads need.

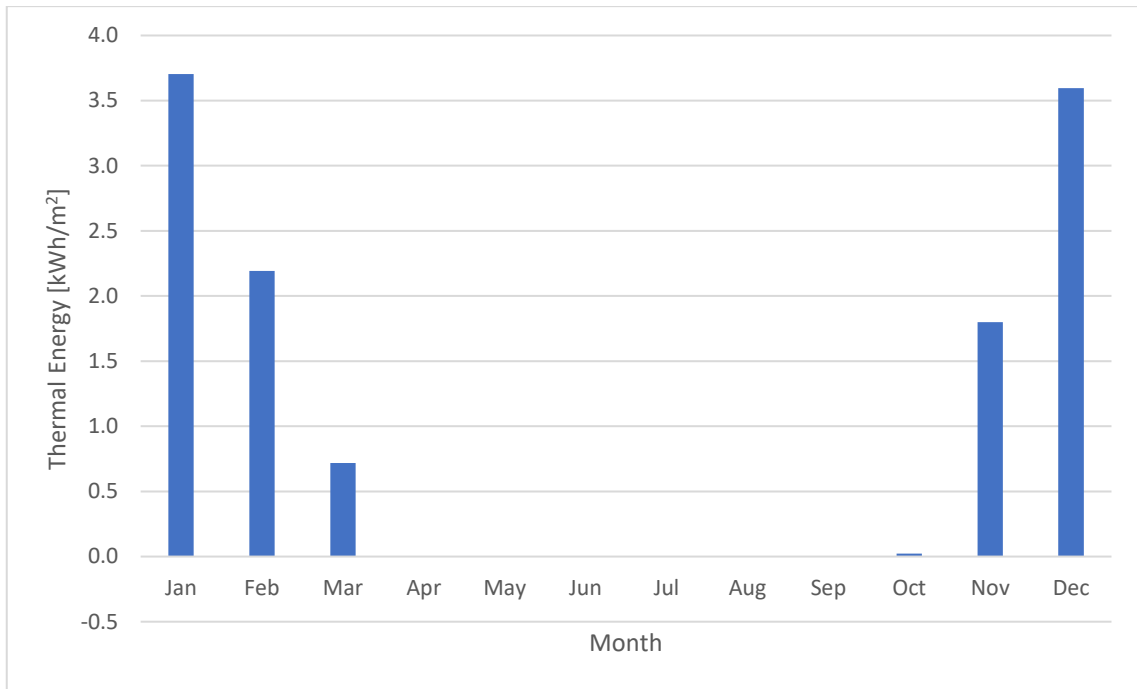


Figure 2.1 Monthly thermal energy needs for floor heating.

Table 16 Simulation-obtained monthly and annual values of the electrical energy consumption of the auxiliaries and of the total of the loads, with detail of their ratio in percent value.

Month	Loads	Auxiliaries	Ratio
Unit	MWh	MWh	%
January	8.9	1.7	19%
February	7.2	1.3	18%
March	6.5	1.1	17%
April	5.5	0.9	17%
May	5.4	1.0	18%
June	5.0	0.9	19%
July	5.0	1.0	19%
August	5.1	1.0	19%
September	5.1	0.9	18%
October	5.6	1.0	17%
November	6.9	1.3	19%
December	8.8	1.7	19%
Year	75.0	13.8	18%

However, in Figure 2.2, it's evident that the energy generated by the photovoltaic panels follows an opposing trend to the monthly loads: it significantly increases during the summer due to the higher available solar irradiation if compared to the winter months.

Also, it can be noticed that, since the PVs generate energy only during the sunny hours and the loads are distributed during the whole day, there is a mismatch between the two which leads to a significantly lower direct consumption of the generated energy with respect the total production, even when the load is higher than the latter. However, as shown in Table 17, the high winter loads lead to the direct consumption of 40-50% of the

generated energy during the heating period, that drops to around 30% during the summer. At the same time, the direct consumption of PV energy represents less than 30% of the electrical energy need during the winter, topping the ratio of around 60% in the summer months.

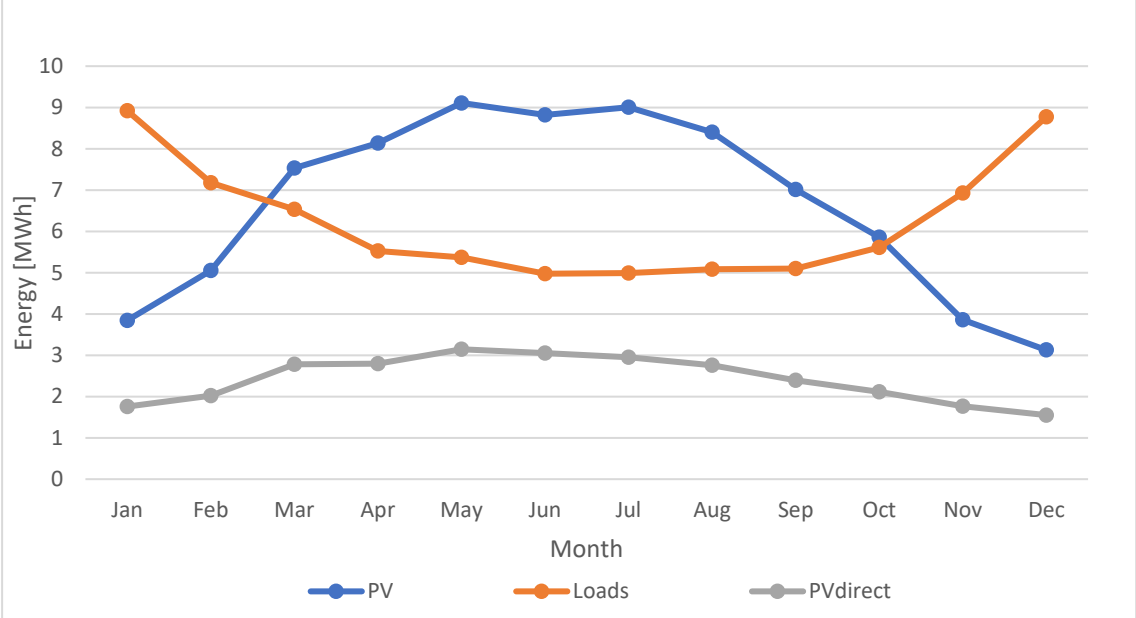


Figure 2.2 Monthly comparison of the electrical energy need due to the loads and the PV energy production and direct consumption.

Table 17 Ratio of the PV direct consumption with respect to the total PV production and the need for the electrical loads.

Month	PV _{direct} /PV _{tot}	PV _{direct} /Loads
Unit	%	%
January	45.8%	19.7%
February	40.0%	28.2%
March	36.9%	42.6%
April	34.4%	50.7%
May	34.5%	58.6%
June	34.6%	61.4%
July	32.8%	59.2%
August	32.8%	54.2%
September	34.1%	46.9%
October	36.1%	37.7%
November	45.7%	25.4%
December	49.6%	17.7%
Year	36.5%	38.8%

In the end, even if the combination of high efficiency building envelope and thermal HVAC plant with a large number of PV modules brings the building to generate 79.8 MWh from solar energy over one year, that is greater than the loads need and means that the building can be considered a Net-Zero Energy Building (NZEB), only 36.5% of the generated energy, representing 38.8% of the electrical need, is directly used.

As a consequence of this, it is clear that installing a storage system is fundamental for such a building, in order to store the PV overproduction and shift its consumption during the periods when the need is significantly higher than the generation. Indeed, Table 18 shows that, using the reference storage system, it is possible to directly use or store 86.7% of the energy produced by the photovoltaic panels, with peaks of more than 95% during those winter periods in which the storage is often emptied due to the presence of a very high electrical need, hence there is often enough available capacity to store the PV generation. In this way, the use of the on-site renewable energy to cover the loads need raises to 57.8% over one year, achieving top values around 80% during the summer, due to the contemporary presence of a lower electrical need.

Table 18 Ratios of the energy directly used from PV or sent to the storage with respect to the total PV production and of the energy directly used from PV or reobtained from the storage with respect to need for the electrical loads.

Month	$PV_{\text{direct consumption + to storage}}/PV_{\text{tot}}$	$PV_{\text{direct consumption + from storage}}/Loads$
Unit	%	%
January	96.4	28.6
February	93.1	41.9
March	92.7	64.1
April	88.0	75.0
May	89.9	80.4
June	92.7	81.9
July	64.3	81.2
August	71.8	78.1
September	88.8	75.0
October	92.6	70.9
November	96.2	43.2
December	97.8	25.8
Year	86.7	57.8

However, by observing the monthly plot of Figure 2.3, it can be seen that, during the winter, the electrical energy is mainly imported from the grid. Since this happens when almost all the energy produced with photovoltaic panels is stored, the cause for this must be ascribed to the behaviour of the storages.

As shown in Table 19 and in Table 20, the ratio between the energy obtained by the storage discharge and that consumed for charging it depicts a different behaviour for the batteries and for the hydrogen storage system: the BESS have an almost constant ratio every month and on a yearly basis, the hydrogen storage system has different values over the year. From this, it can be concluded that the capacity of the batteries allows them to be used only as short-term storage and that the value of the ratio, that is 88%, is hence their average round-trip efficiency.

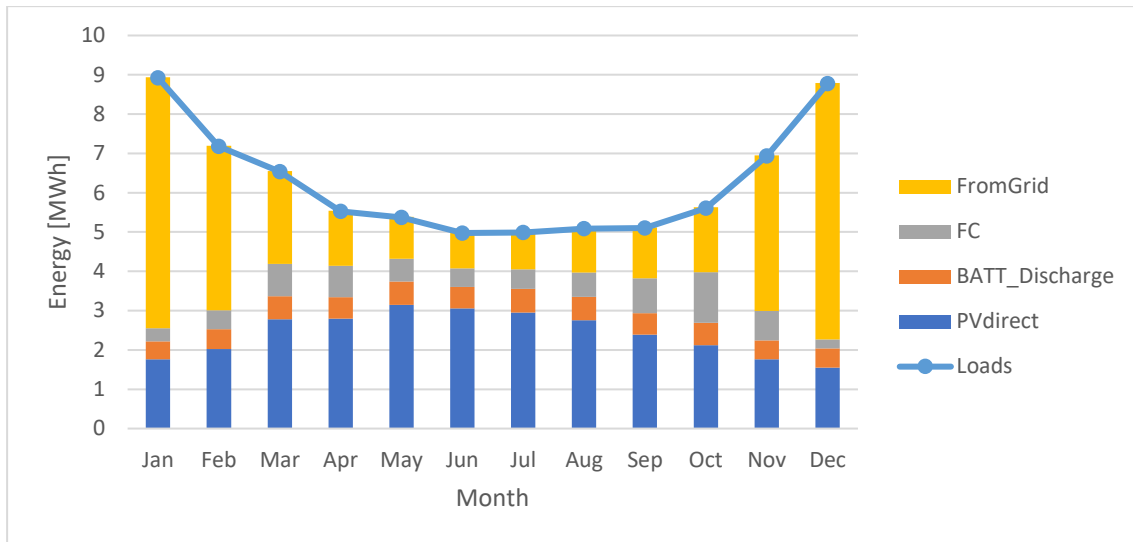


Figure 2.3 Monthly share of the loads need distributed by source used to produce the electrical energy.

On the contrary, the two central columns of Table 20, highlighting the mass of hydrogen produced by the electrolyzers and consumed by the fuel cells, show that the hydrogen is used as short-term storage during the winter and during the summer, while it has more the behaviour of a long-term storage during the spring and the autumn. As a further confirm, since the mass adsorbed is also desorbed on a yearly base, the yearly value can be assumed as the average round-trip efficiency, that is then 24%, and it can be adopted for distinguishing the months in which the HESS is used as a short-term storage, identified as those in which it exhibits the same ratio, from the months when it is used as seasonal storage, having a different value, as shown in the right column of Table 20.

Table 19 Ratio between the energy obtained by the BESS discharge and that consumed for charging it evaluated on a monthly and annual balance and expressed in percent.

Month	$E_{\text{discharge}}/E_{\text{charge}}$
Unit	%
January	88
February	88
March	88
April	88
May	88
June	87
July	87
August	88
September	88
October	88
November	88
December	88
Year	88

Table 20 Monthly and annual balance of the ratio between the energy obtained by the HESS discharge and that consumed for charging it expressed in percent and value of the mass of hydrogen produced by the electrolyzers and consumed by the fuel cells in kg.

Month	$E_{\text{discharge}}/E_{\text{charge}}$	$m_{\text{Electrolysers}}$	$m_{\text{Fuel Cells}}$	Type of use
Unit	%	kg	kg	-
January	24%	25.3	25.3	Short-term
February	23%	37.4	35.9	Short-term
March	23%	62.9	61.5	Short-term
April	21%	66.4	59.8	Mainly short-term
May	13%	77.7	43.2	Long-term
June	10%	79.9	35.1	Long-term
July	23%	38.2	37.1	Short-term
August	24%	46.3	46.8	Short-term
September	28%	57.3	66.7	Mainly short-term
October	48%	47.2	96.1	Long-term
November	53%	25.0	56.1	Long-term
December	24%	16.9	16.9	Short-term
Year	24%	580.5	580.5	-

As a consequence of the change in behaviour, by comparing Figure 2.4 and Figure 2.5, where the dynamic plot of the mass of hydrogen stored in the tank and the monthly share of PV generation are reported respectively, it is possible to notice that, when the maximum state of charge of the hydrogen tank is reached, between June and July, and the electrolyzers use is inhibited or limited to the reproduction of the amount of hydrogen that is consumed by the fuel cells time by time, the energy absorbed by the electrolyzers is subject to a sudden drop, with subsequent peak in the energy immitted in the grid, that continues until the behaviour changes again.

Eventually, as an indicator of the distance of the case studied from the possibility of off-grid operation, it is possible to compare two parameters: the achieved efficiency of the combined storage with both BESS and HESS and the minimum storage efficiency theoretically required by the building to not need grid energy. The first can be calculated from the annual balance, that is reported in Table 21, by taking the inverse ratio of the energy stored from surplus PVs production and the remaining amount subsequently used to fulfil the electricity demands and, since it has been demonstrated that the batteries, despite more efficient, have a limited storage capacity, requiring to use the hydrogen storage system, having a lower efficiency, to accommodate also the daily fluctuations of the electrical need, the obtained value is 36%. The second, instead, requires to evaluate the winter need for additional energy that PVs cannot grant and the summer overproduction with respect to the electrical need, which correspond to the portions of the area between the blue and the orange lines of Figure 2.2: when the orange line indicates a major value than the blue one, the area indicates an electrical need, when the

situation is reversed, it indicates a surplus of PV energy. The obtained values and the calculated theoretical efficiency can be found in Table 22.

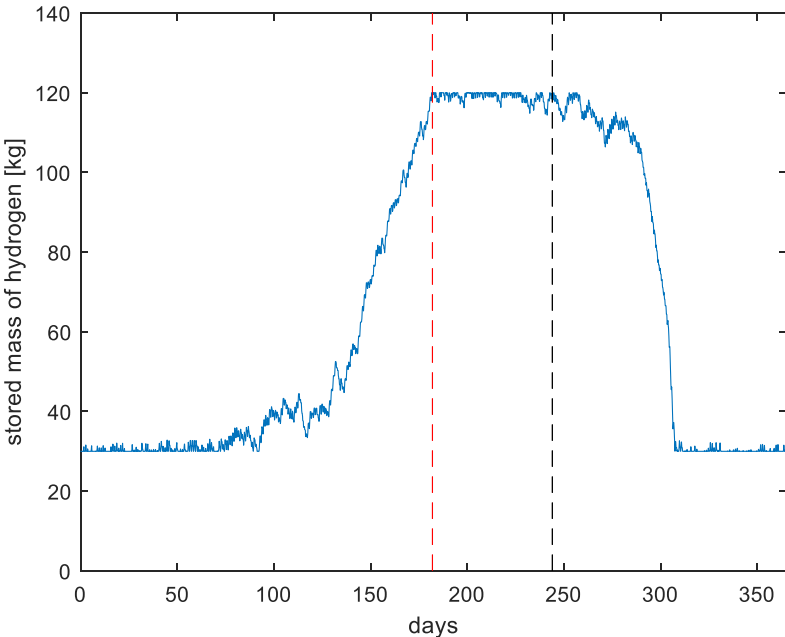


Figure 2.4 Dynamic plot of the mass of hydrogen stored in the tank, with dashed lines indicating July the 1st (red) and September the 1st(black).

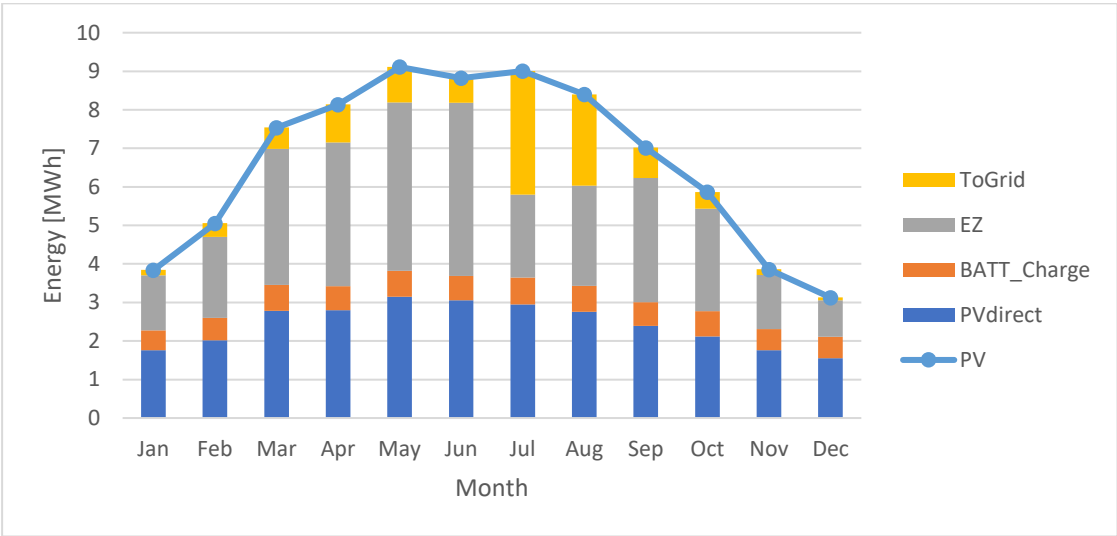


Figure 2.5 Monthly share of the photovoltaic generation.

Table 21 Annual balance of the energy charged and discharged by the BESS and the HESS.

Type of Storage	Unit	Charge	Discharge
BESS	MWh	7.4	6.5
HESS	MWh	32.6	7.7
Total	MWh	40.1	14.3

Table 22 Calculated values for the winter residual need that PV generation cannot cover and the summer PV surplus production.

Parameter	Winter residual need	Summer surplus from PV	Theoretical minimum efficiency
Unit	MWh	MWh	%
Value	15.9	20.7	77

Since the efficiency of the adopted EESS is significantly lower than the minimum theoretical efficiency, the reference case is far away from the possibility of working in off-grid mode, that means also maximising the on-site use of renewables, hence it offers a considerable potential for enhancement.

2.2 Case 2: the variation of the size of the energy storage system

2.2.1 Effect of the variation of the number of the batteries

As shown in Figure 2.6, scaling up the battery energy storage system increases both the average efficiency of the combined storage system and the use of the self-produced energy, thanks to the priority that this has on the hydrogen system. In fact, by observing the more detailed energy plot of Figure 2.7, it can be seen that, while the energy stored by the batteries naturally increases, the consequent reduction of the energy imported from the grid is only partial, since the energy consumed by the electrolysers is reduced as well.

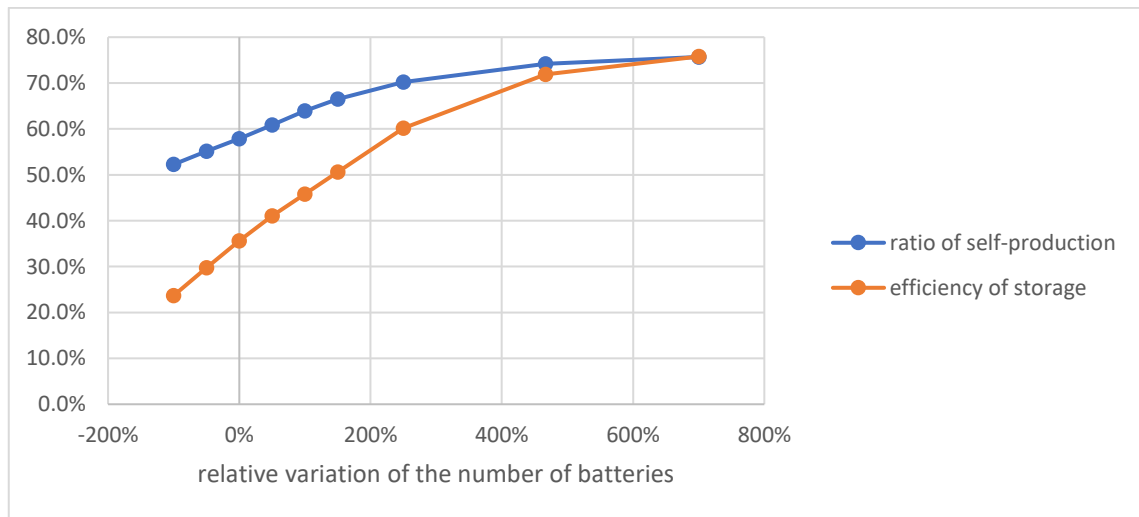


Figure 2.6 Ratio of the total electrical need that is covered with on-site production from renewable energy and efficiency of the combined storage system with batteries and hydrogen storage expressed in percent as a function of the relative variation of the number of the batteries.

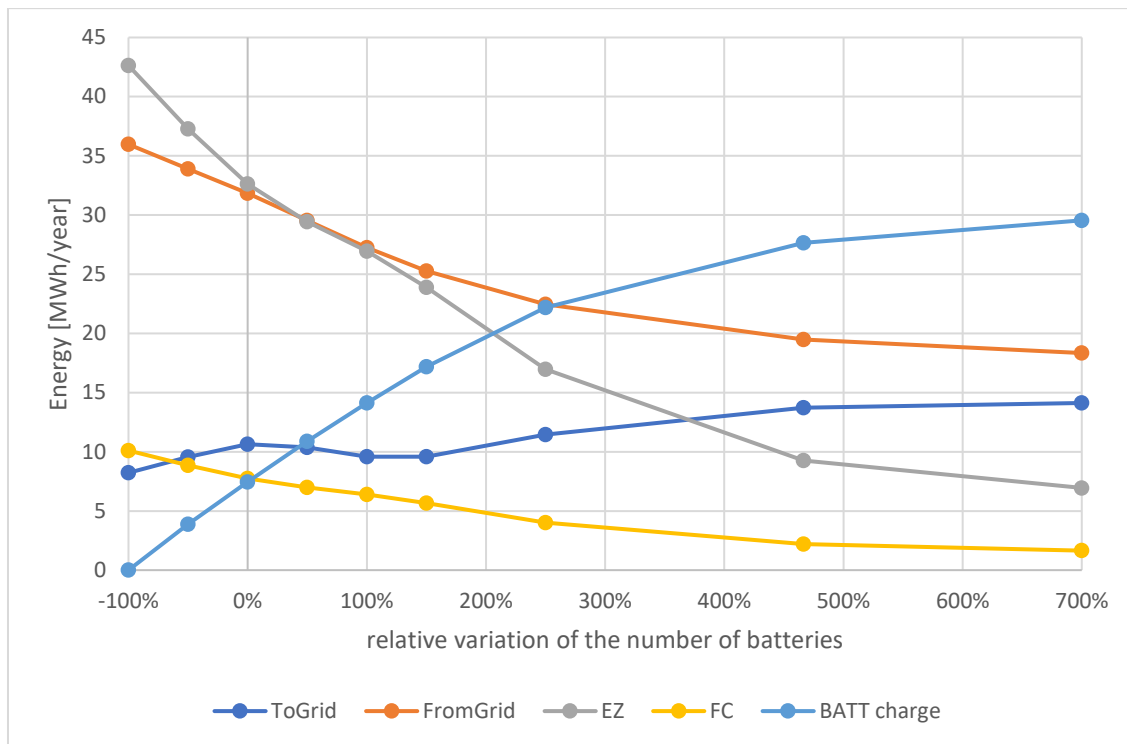


Figure 2.7 Electrical energy exchanged from and to the grid, consumed by the electrolyzers, generated by the fuel cells and used for charging the batteries as a function of the relative variation of the number of the batteries.

However, the reduction of the use of the hydrogen system in favour of a major utilisation of the batteries also exhibits a particular behaviour: a region in which it does not produce an increment in the energy sent to the grid, followed by a new increase and a more rapid decrease in the use of the electrolyzers can be observed. The reason is the switch in the type of use of the hydrogen storage system, which often has to manage the daily fluctuations of the electrical energy need, when the battery capacity is low, and can be employed more for a seasonal use, when the latter is sufficiently increased.

As proof of this, in Figure 2.8 and in Figure 2.9 the monthly ratio between the discharged and charged energy for the BESS and for the HESS is reported respectively: while, for the BESS, it is almost always similar to their efficiency, calculated in Section 2.1, for the HESS this is not true and, in some months, it is not even possible to plot it, because the batteries store all the available PV production, hence the electrolyzers are not used, and the denominator is zero.

This is confirmed also by the comparison of the dynamic plot of the stored mass of hydrogen in the case of the largest considered BESS and in the reference case: as shown in Figure 2.10, with a bigger battery storage, after the transition region, there are lower daily fluctuations. However, it can also be observed that the difference between the cases

+467% and +700% in the dynamic plot of the hydrogen stored mass is minimal, indicating that in both cases the hydrogen system stores almost the maximum energy that the batteries cannot store compatibly with its power limits.

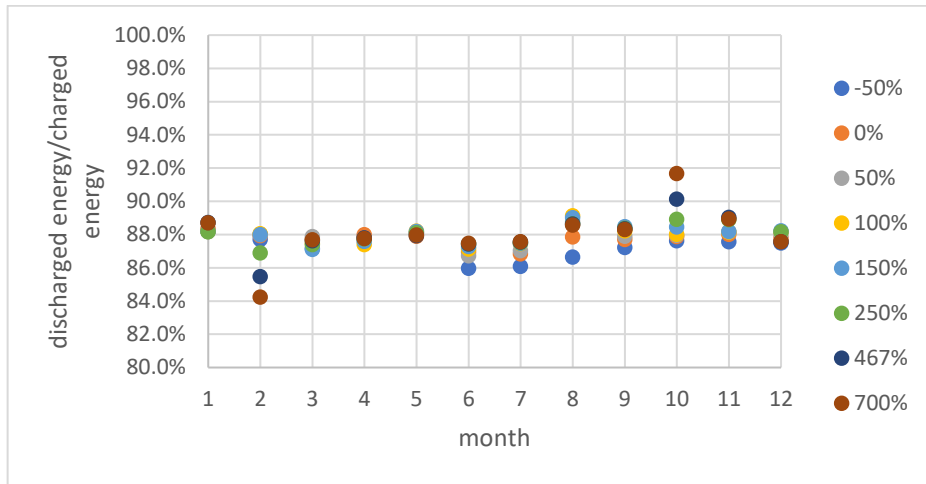


Figure 2.8 Monthly percent ratio between the discharged and charged energy for the BESS expressed as a function of the different simulated sizes of the latter.

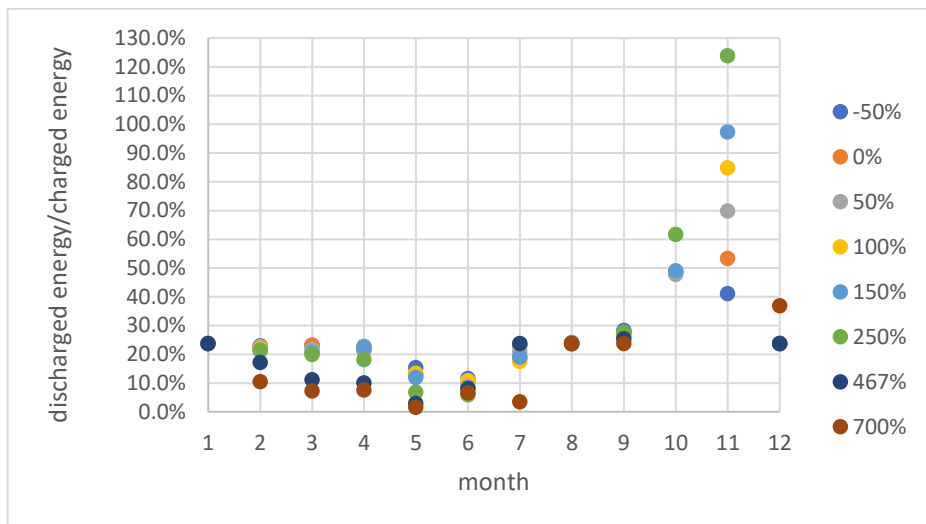


Figure 2.9 Monthly percent ratio between the discharged and charged energy for the HESS expressed as a function of the different simulated sizes of the latter.

Eventually, it is important to notice that the ratio of the self-produced energy of Figure 2.6 is subject to an asymptotic trend. Despite this indicates that the non-ideal behaviour of the batteries, which have both power and capacity limits, does not allow the system to work in off-grid mode unless oversizing the batteries too much, it must be also pointed out that, since in Figure 2.7 the energy immitted into the grid is not null even in the last case, and is actually growing with the size of the BESS thanks to the increase in the efficiency, and in Figure 2.10 the stored hydrogen mass rapidly both reaches the maximum during the spring and finishes during the autumn, a bigger tank would help

with increasing the energy self-production, even if it would also reduce the efficiency of the combined B&H ESS due to an increased use of the hydrogen storage system.

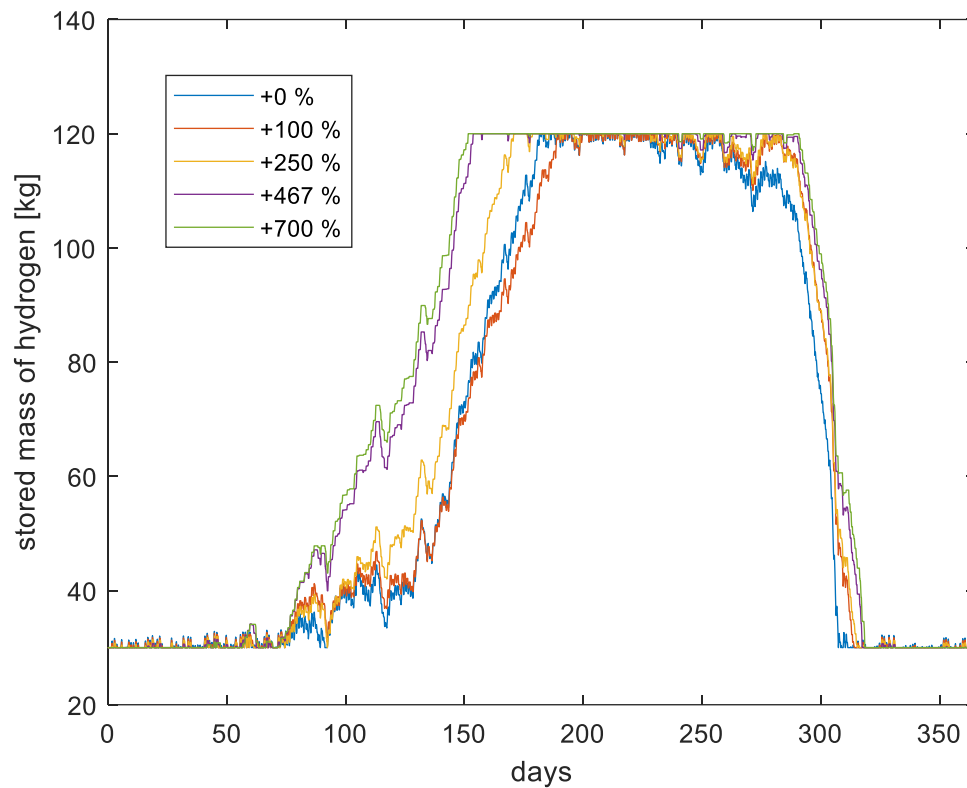


Figure 2.10 Dynamic plot of the mass of hydrogen stored in the MH tank in the case of the largest considered BESS and in the reference case.

2.2.2 The variation of the size of the hydrogen storage system

Since it has been demonstrated that the hydrogen system has a low efficiency, it is fundamental to use it more as a seasonal storage rather than as a daily one. However, the size of the system and the proportions between the electrolysers, the metal hydride storage tank and the fuel cells play an important role in its final exploitation potential.

Respectively in Figure 2.11 and in Figure 2.12, the ratio of the energy self-produced from PV with respect to the total electrical need and the average efficiency of the combined battery and hydrogen energy storage system are plotted on a yearly balance and as function of the relative variation of the three parameters, namely the size of the metal hydride storage tank, the number of the electrolysers and the number of the fuel cells.

In all the three cases, it can be noticed that the increase of the considered parameter has the effect of reducing the efficiency of the combined energy storage system to about 35% and raising the ratio of the consumed energy that is self-produced by the direct use or the

storage of the PV generation to around 60%, hence it means that increasing these parameters has the effect of increasing the use of the hydrogen storage system.

However, it can be also seen that both the indexes reach a limit value, which is followed by a constant trend. In order to explain it, the effect of the change of the three parameters on the dynamic plot of the stored mass of hydrogen has been analysed.

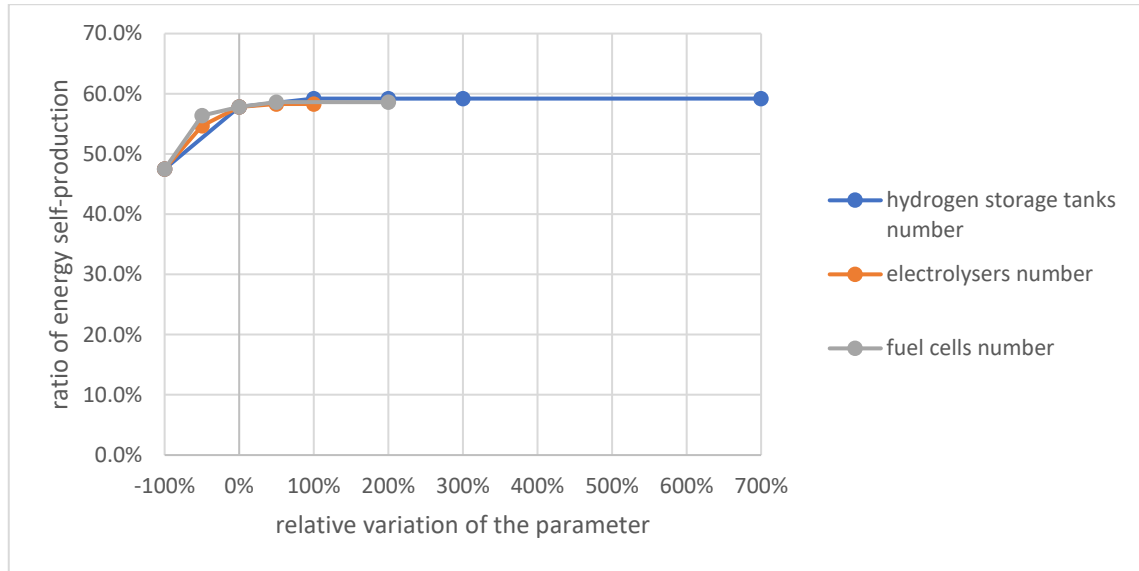


Figure 2.11 Ratio of the energy self-produced from PV with respect to the total electrical need evaluated on a yearly balance and expressed as function of the relative variation of the number of hydrogen storage tanks, electrolyzers and fuel cells.

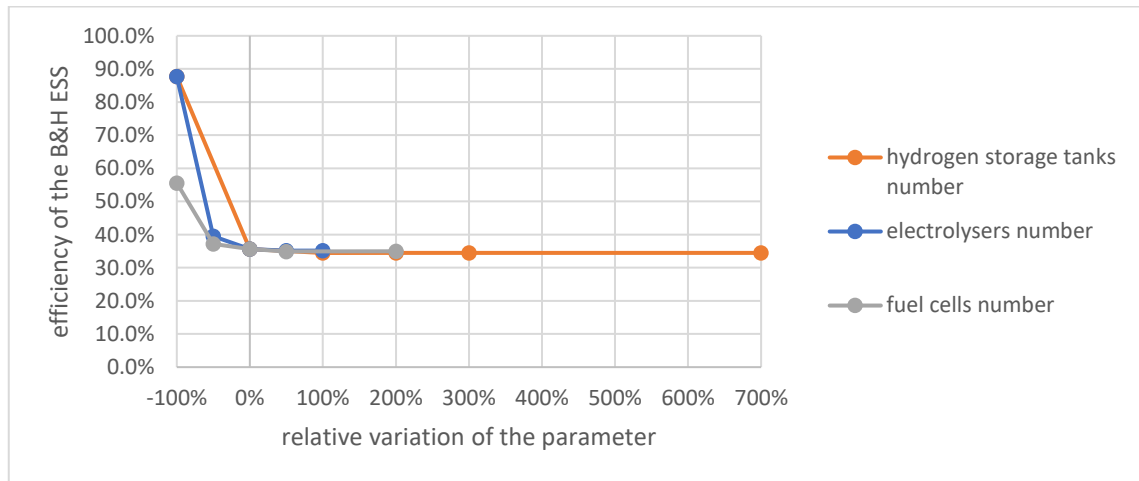


Figure 2.12 average efficiency of the combined battery and hydrogen energy storage system on a yearly balance and expressed as function of the relative variation of the number of hydrogen storage tanks, electrolyzers and fuel cells.

In Figure 2.13, it has been represented for the reference case and the cases +100% and +200% of the size of the hydrogen storage tank and it can be noticed that the capacity is completely used only in the reference case, while in the other cases the mass of the stored hydrogen never reaches the maximum acceptable value. Also, the trends are parallel,

hence the electrolyzers and the fuel cells respectively produce and consume the exact same mass of hydrogen independently from the storage size change. This means that, by increasing the size of the hydrogen tank and not changing the number of the electrolyzers, the limits in the power that these can absorb are the main constraint in the use of the HESS.

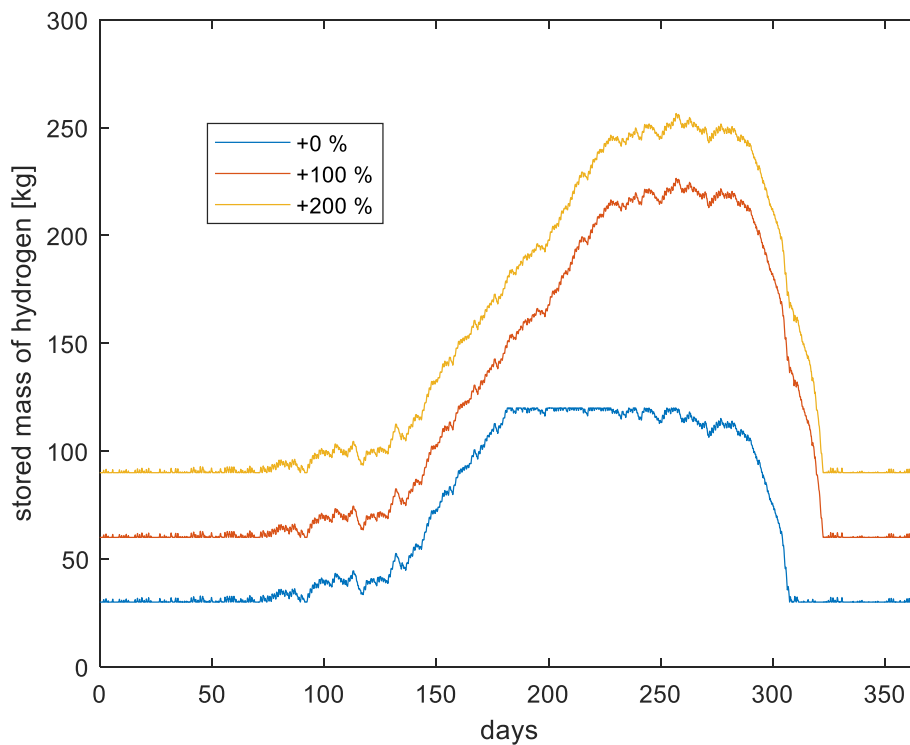


Figure 2.13 Dynamic plot of the stored mass of hydrogen for the reference case and the cases +100% and +200% of the size of the hydrogen storage tank.

When the changing parameter is the number of the electrolyzers, as shown in Figure 2.14 for the reference case and the cases -50%, +50% and +100%, it can be noticed that the storage tank does not fill up in the -50% case and progressively does it sooner with the growing number of the electrolyzers. At the same time, it can be observed that there is a delay also in the autumnal phase of prevalent discharge of the tank. This means that the HESS gains flexibility in terms of maximum charging power thanks to the larger number of electrolyzers. Also, since a major power means a greater amount of produced hydrogen, the additional flexibility with the increasing number of the electrolyzers is accompanied also by a higher amplitude of the oscillations when the HESS is used as daily storage.

However, due to the fact that the maximum mass of hydrogen that can be stored is not increased and neither it is the number of fuel cells, the additional energy that can be absorbed after an increase of 50% is neglectable.

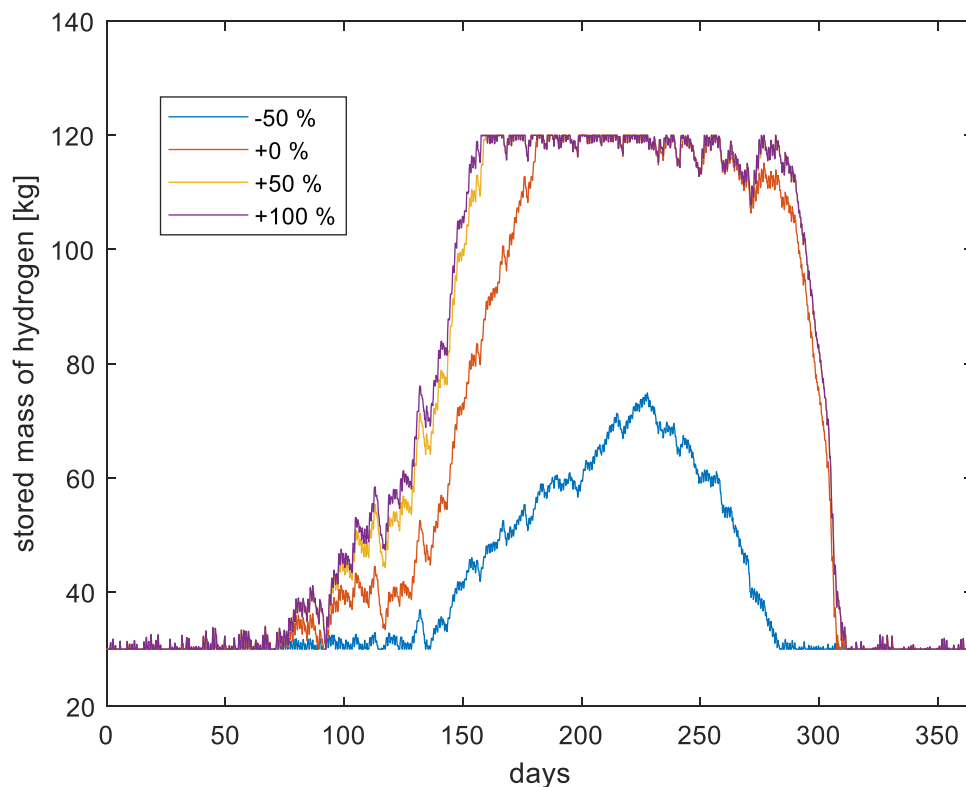


Figure 2.14 Dynamic plot of the stored mass of hydrogen for the reference case and the case -50%, +50% and +100% of the number of the electrolyzers.

Finally, in Figure 2.15, the dynamic plot of the stored mass of hydrogen can be observed for the reference case and the cases -50%, +50% and +200% of the number of the fuel cells. In this plot, it can be noticed that during the use of the HESS as short-term storage, the amplitude of the oscillations is higher with the growing number of the fuel cells, hence the flexibility in the discharge phase is raised. This leads also to a slower filling of the hydrogen tank during the spring, as the fuel cells can discharge it more often and has another great drawback with respect to the necessity of using the hydrogen as a seasonal storage system: the storage tank is emptied earlier during the autumn, leading to a longer period during the winter in which the stored mass of hydrogen is at the minimum value. Hence, the number of the fuel cells should be raised only by increasing also the size of the hydrogen storage tank.

All in all, it can be concluded that, by increasing the size of the metal hydrate storage tank, the number of the electrolyzers and the number of the fuel cells, the whole hydrogen storage system is more used, with the main limit to its energy absorption and release, and hence in the performance indicators of Figure 2.11 and Figure 2.12, being the fact of modifying only one of the parameters at once, that thus should be avoided. In particular,

by modifying the size of the tank, the electrolyzers can become insufficient to fill it up, hence leaving part of the increased capacity not used; by increasing the number of the electrolyzers, the tank is full earlier and emptied later, hence following better the PV surplus generation, but, since the size of the tank limits the benefit, this requires to be scaled up as well; a larger number of fuel cells, finally, helps to follow better the electrical energy need, but it might also require more electrolyzers to be sure that the hydrogen storage is filled up during the spring and it causes the HESS to be emptied more rapidly during the autumn, hence it should be done only with a larger hydrogen storage tank as well, to avoid having an empty HESS during the winter.

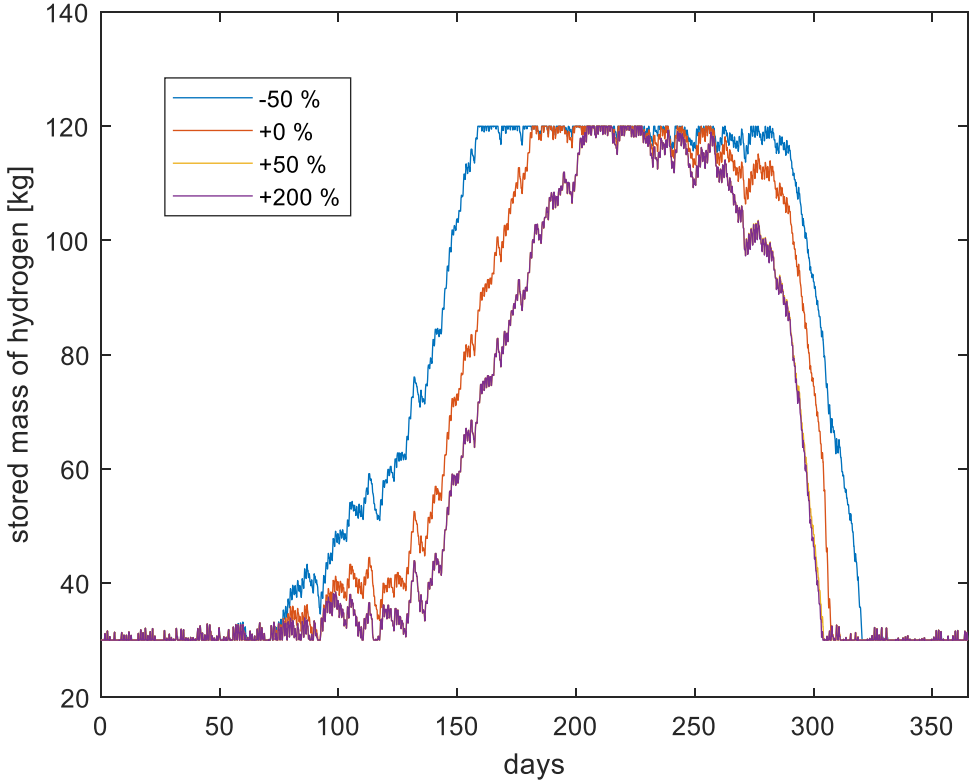


Figure 2.15 Dynamic plot of the stored mass of hydrogen for the reference case and the case -50%, +50% and +200% of the number of the fuel cells.

2.3 Case 3: the variation of the number of the photovoltaic panels

A strategy to enhance the self-production of the energy for the electrical need could be the increase of the number of the photovoltaic panels. This, in particular, cannot be done on the building façades due to fire-safety restrictions, hence it has been done making the hypothesis of having an available area nearby the building to install additional PV panels.

In Figure 2.16, the PV generation curve is plotted for the analysed cases, with increasing number of additional panels, and it is compared with the electrical energy need. As expected, increasing the on-site production has the effect of shifting the production curve to higher energy values. Since this means that the area between the two curves in which the PV curve is higher than that of the electricity need becomes larger, while the area in which the latter has a greater value becomes smaller, the efficiency that an ideal energy storage system allowing the building to work in off-grid mode would have been evaluated for the different increases of the PV production by calculating the mentioned areas and the ratio of them. As shown in Table 20, the obtained values are progressively lower, hence the increase of the number of the PV panels is a solution to produce more electrical energy for chosen size of the combined battery and hydrogen energy storage system, in order to match its efficiency.

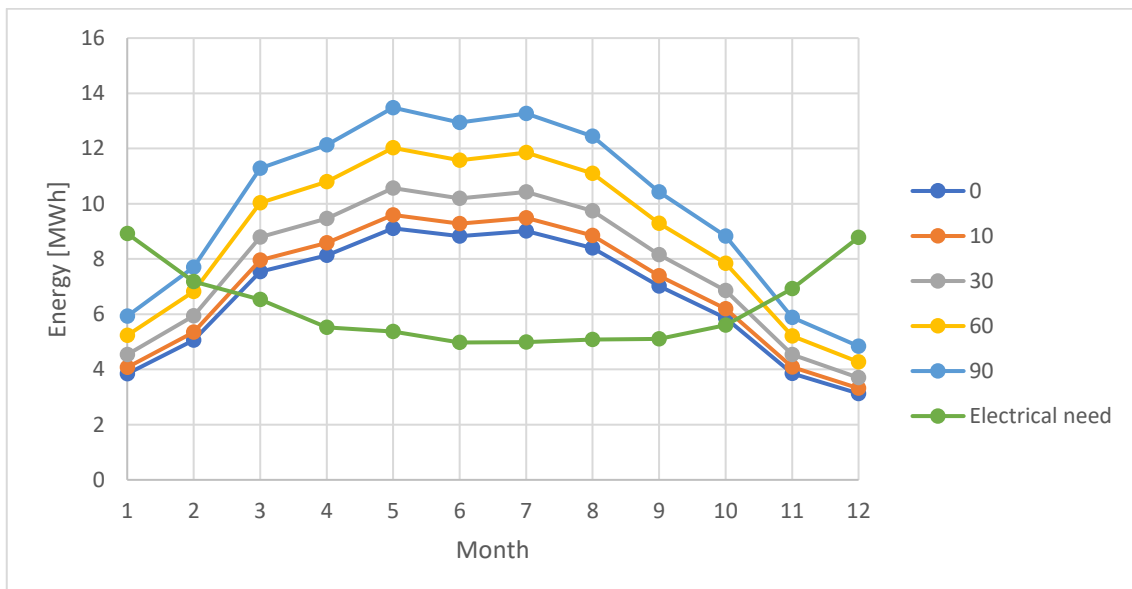


Figure 2.16 Comparison between the electrical need curve and the different PV generation curves obtained increasing number of additional panels.

Table 23 Values of the yearly PV surplus energy and residual electrical energy need and of the calculated theoretical minimum efficiency for off-grid operation for the different cases with increasing number of additional PV panels.

	Unit	Reference case	+10 additional PV panels	+30 additional PV panels	+60 additional PV panels	+90 additional PV panels
Winter residual need	MWh	15.9	24.1	31.0	41.3	52.2
Summer surplus from PV	MWh	20.7	15.0	13.1	10.3	8.0
Theoretical minimum efficiency	%	77	62	42	25	15

However, as shown in Figure 2.17, by calculating the ratio between the energy exported to the grid and the sum of the energy generated by the PVs and imported from the grid in a yearly balance, it is possible to affirm that, by increasing the number of the PV panels

without adapting the size of the storage system, the fraction of the gained enhancement in PV production that is not used directly in the building progressively grows. Consequently, the number of the PV panels must be chosen according to the size of the storage system.

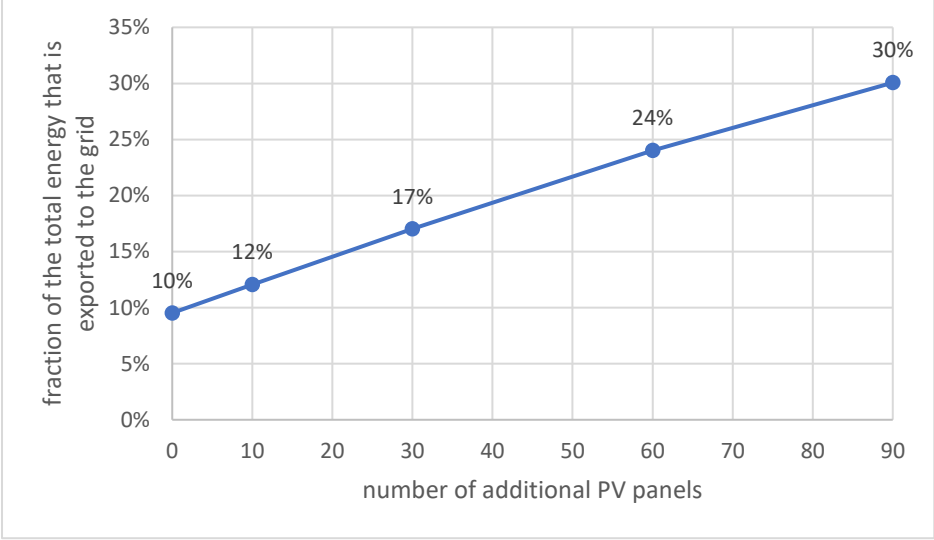


Figure 2.17 Ratio between the energy exported to the grid and the sum of the energy generated by the PVs and imported from the grid in a yearly balance by increasing the number of the PV panels.

CONCLUSIONS

In the context of lowering the environmental impact of the residential buildings, the reduction of the electrical energy imported from the grid is fundamental and installing photovoltaic (PV) panels is a common strategy to produce on-site electricity from renewable energy sources. However, due to the stochastic nature of the solar source, electrical energy storage systems are required to address the inevitable mismatch between the electrical loads and the PV production.

Though battery energy storage systems (BESS) are the most used, since they are affected by self-discharge, this introduces limitations in long-term storage applications and has prompted the exploration of the hydrogen energy storage systems (HESS) as their complement for the seasonal fluctuations of the electrical need. However, since a HESS is usually less efficient than a BESS, the two systems should be sized properly in order to obtain a combined energy storage system that is capable of improving the energy self-production and, at the same time, doing it as much efficiently as possible.

To provide guidance on how to do it, the modifications in the energy performance of a building for different sizes of the electrical components of the HVAC plant, namely the number of the batteries, the number of the hydrogen storage tanks, the number of the electrolyzers, the number of the fuel cells and the number of the photovoltaic panels, have been analysed.

More in detail, a multi-family building that will be built in the city of Innsbruck and will be equipped with PVs and a combined storage composed of batteries and hydrogen storage system has been selected for the study. First of all, the building has been simplified in order to be able to realise a model for it in the MATLAB-Simulink environment using the tool for dynamic simulation carnotUIBK. Subsequently, with the help of the carnot library, the model has been integrated with two subsystems, representing, in a simplified way, the thermal and the electrical parts of the HVAC plant.

Since the model was produced starting from a real project, this has been kept as reference case for the variation of the parameters and analysed for first. In particular, it has been concluded that the building, being very efficient, is indeed a net-zero energy building as it manages to have an annual PV generation of electrical energy higher than its need.

However, it has been noticed also that only less than 36.5% of the produced energy, which is less than 40% of the need, can be directly used from the PVs and thus that the energy storage is fundamental, as it raises the used PV energy to more than 80%, leading to self-producing almost the 60% of the electrical need, already in its initial size. Although there is a benefit, the much lower increase in the self-production of the need with respect to that in the on-site use of the PV-generated energy led to the necessity of evaluating the behaviour of the hybrid energy storage system and its efficiency. The conclusion has been that the total efficiency is 36%, significantly lower than that of the batteries, which is 88%, due to the fact that they are too undersized and hence cause the hydrogen storage system to be used also for the daily fluctuations of the electrical need. In addition, the theoretical minimum efficiency which a storage should have to allow the building to remain disconnected from the grid has been evaluated as 77%, hence it has been declared that the building hybrid storage system should be modified to obtain a higher efficiency value, closer to this one.

The first parameter that has been changed has been the battery capacity. From the results, it has been observed that, since the batteries have the priority of use on the hydrogen system due to their higher efficiency, by increasing their capacity, their use is enhanced and that of the hydrogen reduced, leading to a raised, although stabilizing, ratio of the self-produced electrical need. As a consequence of this, it has been concluded that, although it is not possible to reach the off-grid operation, this is a good strategy to bring the hydrogen storage to a more seasonal use and raise the efficiency of the hybrid energy storage system to values even higher than 77%.

On the contrary, with increasing sizes of the hydrogen storage system, it has been noticed that the self-production of the electrical need raises a bit and the efficiency of the combined storage system lowers a bit. However, as long as the residual amount of the energy that can be stored is limited due to the fact that the use of the batteries is not influenced, the parameters rapidly reach a constant trend, slightly lower than 60% for the self-production of the need and around 35% for the efficiency of the hybrid storage system.

In addition, for the different parameters of the hydrogen storage system, it has been concluded that varying them only one by one is not a good practice. In facts, this, for the case of the storage tank, leads to not having enough electrolysers to fill it up and, for the case of the electrolysers or the fuel cells, it makes possible the gain of an increased

flexibility in the charge and discharge phases, respectively, but, since the size of the tank does not vary and neither the remaining PV surplus energy not absorbed by the batteries does it, in the end, it leads only to a more rapid charge or discharge of the hydrogen tank. In none of the cases, without changing the battery capacity, the hydrogen storage system is used in a more seasonal way.

Eventually, the increase of the number of the PV panels has demonstrated to have the effect of producing more energy from the solar source, hence it is an option to allow the building to work in off grid mode also with a low-efficiency energy storage system. However, since the storage for the present building is not sized to reach the possibility to disconnect it from the grid, here it has in particular the effect of raising the energy exported to the grid, that is not desired in this study. Therefore, it has been stated that the installed number of the PV panels has to be decided only strictly accordingly to a well-defined size, and hence efficiency, of the hybrid energy storage system.

All in all, although this analysis of a multi-family building integrated with a hybrid storage system, including both batteries and a hydrogen energy storage system, furnishes information about the change in behaviour of the storage when the size of its components are varied and hence represents a reliable guidance for deciding which type of interventions applying to obtain a major energy self-production and maintaining an acceptable efficiency, there is still space for improvements.

In particular, since the model represents the hydrogen storage tank in a very ideal way, it does not take into account how much thermal energy is associated to the processes of hydrogen adsorption and desorption. At the same time, if the cooling required by the first of the two might be done with the underground water and the auxiliaries could be neglected, using either an additional heat pump or the main one of the building would be necessary to enhance the hydrogen desorption, leading to an increase in the electrical energy need. A more detailed model for the hydrogen storage tank would allow to understand if this is relevant and how much it worsens the energy performance of the building or if it can be neglected.

AKNOWLEDGMENTS

This study has been made possible by the partnership between the University of Bologna, as sending institute, and the University of Innsbruck, as hosting institute. In particular, a fundamental role must be recognised to the Prof. Ing. Claudia Naldi, from the Thermal Engineering department of Alma Mater Studiorum, University of Bologna, for the role of supervisor of the Master Thesis, and to the Assoc. Prof. Dr.-Ing. Fabian Ochs and the Dr. techn. Mara Magni, MSc, from the Unit for Energy Efficient Building of the University of Innsbruck, as they, in the role of co-supervisors, provided support in the use of the MATLAB-Simulink tool carnotUIBK and shared the considerable expertise that they have accumulated in the field of the dynamic simulation of buildings through years of dedicated practice.

REFERENCES

- [1] International Energy Agency. (2024, February 6th) **Share of total final consumption (TFC) by sector, European Union (EU), 1990-2021.** https://www.iea.org/data-and-statistics/data-tools/energy-statistics-data-browser?country=EU27_2020&fuel=Energy%20consumption&indicator=TFCbySector
- [2] International Energy Agency. (2024, February 6th) **Carbon intensity of industry energy consumption, European Union (EU27), 1990-2021.** https://www.iea.org/data-and-statistics/data-tools/energy-statistics-data-browser?country=EU27_2020&fuel=Energy%20consumption&indicator=CO2Industry
- [3] M.A. Fazal, Saeed Rubaiee (2023). **Progress of PV cell technology: Feasibility of building materials, cost, performance, and stability.** *Solar Energy*, 258, 203-219. DOI: 10.1016/j.solener.2023.04.066
- [4] Rabee M. Reffat, Radwa Ezzat (2023). **Impacts of design configurations and movements of PV attached to building facades on increasing generated renewable energy.** *Solar Energy*, 252, 50-71. DOI: 10.1016/j.solener.2023.01.040
- [5] WanTing Wang, Hongxing Yang, ChangYing Xiang (2023). **Green roofs and facades with integrated photovoltaic system for zero energy eco-friendly building – A review.** *Sustainable Energy Technologies and Assessments*, 60. DOI: 10.1016/j.seta.2023.103426
- [6] Yuejiang Chen, Jiang-Wen Xiao, Yan-Wu Wang, Yuanzheng Li (2023). **Regional wind-photovoltaic combined power generation forecasting based on a novel multi-task learning framework and TPA-LSTM.** *Energy Conversion and Management*, 297. DOI: 10.1016/j.enconman.2023.117715
- [7] Peter D. Lund, Juuso Lindgren, Jani Mikkola, Jyri Salpakari (2015). **Review of energy system flexibility measures to enable high levels of variable renewable electricity.** *Renewable and Sustainable Energy Reviews*, 45, 785-807. DOI: 10.1016/j.rser.2015.01.057

- [8] Felix Cebulla, Jannik Haas, Josh Eichman, Wolfgang Nowak, Pierluigi Mancarella (2018). **How much electrical energy storage do we need? A synthesis for the U.S., Europe, and Germany.** *Journal of Cleaner Production*, 181, 449-459. DOI: 10.1016/j.jclepro.2018.01.144
- [9] J.P. Deane, B.P. Ó Gallachóir, E.J. McKeogh (2010). **Techno-economic review of existing and new pumped hydro energy storage plant.** *Renewable and Sustainable Energy Reviews*, 14(4), 1293-1302. DOI: 10.1016/j.rser.2009.11.015
- [10] Shafiqur Rehman, Luai M. Al-Hadhrami, Md. Mahbub Alam (2015). **Pumped hydro energy storage system: A technological review.** *Renewable and Sustainable Energy Reviews*, 44, 586-598. DOI: 10.1016/j.rser.2014.12.040
- [11] Shaoquan Lin, Tao Ma, Muhammad Shahzad Javed (2020). **Prefeasibility study of a distributed photovoltaic system with pumped hydro storage for residential buildings.** *Energy Conversion and Management*, 222. DOI: 10.1016/j.enconman.2020.113199
- [12] Marc Beaudin, Hamidreza Zareipour, Anthony Schellenberglobe, William Rosehart (2010). **Energy storage for mitigating the variability of renewable electricity sources: An updated review.** *Energy for Sustainable Development*, 14(4), 302-314. DOI: 10.1016/j.esd.2010.09.007
- [13] Rebecca E. Ciez, J.F. Whitacre (2016). **The cost of lithium is unlikely to upend the price of Li-ion storage systems.** *Journal of Power Sources*, 320, 310-313. DOI: 10.1016/j.jpowsour.2016.04.073
- [14] Yuchen Yang, Zhen Wu, Jing Yao, Tianlei Guo, Fusheng Yang, Zaoxiao Zhang, Jianwei Ren, Liangliang Jiang, Bo Li (2024). **An overview of application-oriented multifunctional large-scale stationary battery and hydrogen hybrid energy storage system.** *Energy Reviews*, 3(2). DOI: 10.1016/j.enrev.2024.100068
- [15] Qusay Hassan, Sameer Algburi, Aws Zuhair Sameen, Hayder M. Salman, Marek Jaszczur (2024). **Green hydrogen: A pathway to a sustainable energy future.** *International Journal of Hydrogen Energy*, 50(B), 310-333. DOI: 10.1016/j.ijhydene.2023.08.321
- [16] Torbjørn Egeland-Eriksen, Amin Hajizadeh, Sabrina Sartori (2021). **Hydrogen-based systems for integration of renewable energy in power systems:**

- Achievements and perspectives.** *International Journal of Hydrogen Energy*, 46(63), 31963-31983. DOI: 10.1016/j.ijhydene.2021.06.218
- [17] Pietari Puranen, Antti Kosonen, Jero Ahola (2021). **Technical feasibility evaluation of a solar PV based off-grid domestic energy system with battery and hydrogen energy storage in northern climates.** *Solar Energy*, 213, 246-259. DOI: 10.1016/j.solener.2020.10.089
- [18] Rajan Kumar Jaysawal, Suprava Chakraborty, D. Elangovan, Sanjeevikumar Padmanaban (2022). **Concept of net zero energy buildings (NZEB) - A literature review.** *Cleaner Engineering and Technology*, 11. DOI: 10.1016/j.clet.2022.100582
- [19] Passive House Institute (February 7th). **About Passive House. Passive House requirements.** https://passivehouse.com/02_informations/02_passive-house-requirements/02_passive-house-requirements.htm
- [20] MathWorks (February 9th). **MATLAB – Il linguaggio del calcolo tecnico.** <https://it.mathworks.com/products/matlab.html>
- [21] MathWorks (February 9th). **Simulink – Simulazione e progettazione Model-Based.** <https://it.mathworks.com/products/simulink.html>
- [22] Universität Innsbruck (February 9th). **carnotUIBK Toolbox for MATLAB Simulink.** <https://www.uibk.ac.at/bauphysik/forschung/carnotuibk/index.html.en>
- [23] GitHub – MaraMagni/carnotUIBK_ME (February 9th). **carnotUIBK – The MATLAB Toolbox for thermal building simulations.** https://github.com/MaraMagni/carnotUIBK_ME
- [24] MathWorks (February 9th). **Carnot Toolbox.** <https://it.mathworks.com/matlabcentral/fileexchange/68890-carnot-toolbox>
- [25] sciebo (February 9th). **Files.** <https://fh-aachen.sciebo.de/index.php/s/0hxeb0iIJrui3ED>
- [26] Meteotest (February 15th). **Meteonorm Software.** <https://meteonorm.com/en/>
- [27] APCS – Power Clearing & Settlements (February 15th). **Synthetische Lastprofile.** <https://www.apcs.at/de/clearing/technisches-clearing/lastprofile>
- [28] ÖNORM H 5056-1: **Energy performance of buildings - Part 1: Energy use for heating systems.** Austrian Standards International, 2023. [Online] Available at:

https://lesesaal.austrian-standards.at/action/de/private/details/1301122/OENORM_H_5056-1_2023_10_01

[Last accessed: January 10th 2024]

[29] Universität Kassel (February 15th). **Downloads.** <https://www.uni-kassel.de/maschinenbau/institute/thermische-energietechnik/fachgebiete/solar-und-anlagentechnik/downloads>

[30] Ralf Dott, Michel Y. Haller, Jörn Ruschenburg, Fabian Ochs and Jacques Bony (2013). **The Reference Framework for System Simulations of the IEA SHC Task 44 / HPP Annex 38. Part B: Buildings and Space Heat Load.** A technical report of subtask C. Report C1 Part B. DOI: 10.13140/2.1.2221.4727